HHS Public Access

Author manuscript

Annu Rev Vis Sci. Author manuscript; available in PMC 2016 March 10.

Published in final edited form as:

Annu Rev Vis Sci. 2015 November ; 1: 19–50. doi:10.1146/annurev-vision-082114-035357.

Adaptive optics ophthalmoscopy

Austin Roorda and
University of California, Berkeley

Jacque L. Duncan
University of California, San Francisco

Abstract

This review starts with a brief history and description of adaptive optics (AO) technology, followed by a showcase of the latest capabilities of AO systems for imaging the human retina and an extensive review of the literature on where AO is being used clinically. The review concludes with a discussion on future directions and guidance on usage and interpretation of images from AO systems for the eye.

Keywords

adaptive optics; ophthalmoscopy; retina; scanning laser ophthalmoscopy; fundus camera

1.0 Introduction

The use of adaptive optics (AO) converts an ophthalmoscope into a microscope, allowing visualization and optical access to individual retinal cells in living human eyes in ways not possible before (Liang et al 1997). This microscopic access is driving a paradigm shift in how we use ophthalmoscopy for the study of vision and visual dysfunction.

AO is a technology that was originally developed by astronomers to sharpen images by compensating the blur-inducing optical aberrations caused by turbulence within the earth's atmosphere. In the field of vision science, AO compensates for optical aberration in the eye's optics and can be applied to any ophthalmoscope modality, including full-field fundus cameras, scanning laser ophthalmoscopes (SLO), and optical coherence tomography (OCT) systems. This review concerns the first two modalities only since they are the ones that have yielded the majority of clinical research published to date. Also, OCT has had such a profound impact in the field of ophthalmology that it warrants its own dedicated review.

AO technology for ophthalmoscopy is relatively young, and new technical developments, new applications and new approaches to the analysis, interpretation and presentation of results are appearing monthly. Considering this, the review will place as much emphasis on emerging applications of AO technology that are relevant for clinical ophthalmic applications (Sec 3) as on what has already been learned (Sec 4). The aim is that this review will offer guidance on exciting new clinical directions that AO users and developers should consider. Another aim is to point out some areas of AO research, specifically those related to image analysis and interpretation, which beg for more attention (Sec 5).

2.0 What is AO?

An AO system involves two important steps: measuring the optical imperfections of the eye and compensating them. This compensation is generally done over the largest pupil size possible to maximize the numerical aperture (see inset).

There are several ways to measure aberrations in the eye, but the Shack-Hartmann Wavefront Sensor (SHWS) is the approach that made AO possible and it seems, by all accounts, to be the best available approach to measure aberrations in the human eye. Junzhong Liang was the first to develop a SHWS for the human eye as part of his PhD research the University Heidelberg Germany with Josef Bille (Liang et al 1994) and it was further refined at the University of Rochester (Liang & Williams 1997).

Recognizing the enabling potential of SHWS technology for ophthalmic applications, Liang and Donald Miller, led by David Williams, built the world's first AO retinal camera (Liang et al 1997). The key technology was a deformable mirror which could be shaped in a way to give it an aberration equal and opposite the eye as measured by the SHWS. Thus, the aberrations in the beam of light emerging from the eye would be effectively cancelled by the aberrations of the mirror. For more details on AO technology, the reader can refer to the following chapters and reviews (Miller & Roorda 2009, Porter 2006, Roorda 2011, Williams 2011). The benefits of using AO for ophthalmoscopy were immediately realized, as the images to come out of the world's first AO fundus camera showed the first resolved images of arrays of human cone photoreceptors (Liang et al 1997).

It is no coincidence that the fundus camera was the first ophthalmic imaging modality adopted for AO. Fundus cameras employ simple optical principles and involve little more than a camera forming an image on a light-sensitive film (or CCD) of the light emerging from the retina through the eye's optics. Implementing AO is only a matter of placing the corrector at an appropriate location between the camera and the eye. It is important to note here that any ophthalmic device that involves having to pass light into or out of the eye could benefit from AO. The benefit is not only limited to ophthalmoscopes, but vision testing systems as well (Fernandez et al 2009, Guo et al 2008, Roorda 2011, Sawides et al 2010, Schwarz et al 2014, Yoon & Williams 2002). One ophthalmic imaging technology that is very well-suited for AO is the scanning laser (or light) ophthalmoscope (SLO). Invented in 1980 by Robert Webb (Webb et al 1980), the SLO forms an image over time by continually recording and logging the light scattered from a single focused spot on the retina as it is scanned across the retina, generally in a raster pattern. SLOs are well-suited to record movies of the retina at video rates and can be used a vast number of ways. The most common mode of imaging is confocal imaging, in which a small aperture (confocal pinhole) positioned close to the detector and which is optically conjugate to the focused spot on the retina, is used. The confocal pinhole blocks scattered light from reaching the detector except that which comes from near the plane of focus. The use of this confocal pinhole thereby enables optical sectioning, which is the primary advantage of confocal microscopes over conventional light-field microscopes. In the human eye the confocal pinhole allows for some optical sectioning (albeit not close to the axial sectioning ability of OCT) but it also provides high contrast images of the structure of interest.

The first application of AO to an SLO was by (Roorda et al 2002). In that paper, the video-rate imaging and confocal advantages of the SLO were demonstrated in the measurement of blood cell velocity and rudimentary optical sectioning. The complexity of the design and the reliance on partially coherent light sources (Putnam et al 2010) was a compromise for using SLO in the first years, but the availability of better light sources (Zhang et al 2006) and innovative optical design (Dubra & Sulai 2011) have overcome most of those early limitations. Today, AOSLOs in research labs are producing *en face* retinal images with higher contrast and resolution than any other imaging modality. In fact, it appears that the best AOSLOs have achieved a resolution that is effectively at the diffraction-limit for eyes with clear optical media (Dubra et al 2011).

The implementation of AO in an ophthalmoscope is only the first step in realizing its full range of benefits. Consider, for comparison, the field of microscopy. In today's laboratories, the use of a microscope to look at scattered or transmitted light from biological specimens represents a small fraction of its applications. Almost every use of the microscope today employs contrast agents, fluorescent labels, or innovative illumination and detection schemes. The arsenal of tools available to the microscopist is expanding. While standard approaches involving the recording of scattered light from the retina have proven useful for both fundus camera and SLO modalities, the reflected or scattered light does not provide specific information about a retinal cell's function or its health. Even the simple notion that a visible cone is a healthy cone or an invisible cone indicates visual dysfunction has been questioned (Wang et al 2015). However, this review will show that there is an expanding array of more innovative uses of AO technology within these modalities, and we've witnessed only the very beginnings of what can be done. Put simply, AO offers microscopic optical access, and it is up to the ophthalmoscopist to determine how to employ that access.

3.0 State of the Art in AO Imaging Technology

This section showcases the capabilities of today's AO systems and is intended to make it clear that AO is a developing technology. Had the review focused solely on clinical applications, it would have failed to give the reader an appreciation of AO's potential capabilities. Actual clinical studies can be complicated with an emerging technology. The time with a patient is limited, the patients and the operators are often less familiar with the technology than those who build them, and many patients may not have optimal fixation, lens clarity, tear film stability or patience, all of which can compromise quality data collection. Nevertheless, AO is already having an impact in ophthalmology as Sec. 4 will show.

3.1 Imaging Structure

Visualizing microscopic structure in the retina requires a combination of resolution, contrast and a sufficient signal to noise ratio (SNR) (see inset for a definitions). AO offers the resolution in all cases, but sufficient contrast and SNR is reached in a number of different ways. In this section, we showcase the best images of all the retinal structures imaged to date in healthy eyes using all the current AO imaging modalities, with the exception of AO-optical coherence tomography. Most imaging modalities have been used on humans but, for those images which are from animals, an inset is added to the figure to indicate the species.

Nerve Fiber Layer—Axons of the ganglion cells traverse across the surface of the retina, forming the nerve fiber layer. The NFL is a relatively strong source of back-scatter and its microstructure has been resolved with confocal AOSLO imaging (Huang et al 2014, Takayama et al 2012) and AO fundus cameras (Ramaswamy et al 2014). Fig. 1 shows a confocal AOSLO image of discrete, individual, nerve fiber bundles originating from the temporal raphe. Closer looks at this structure will help to provide a better understanding of, and an ability to monitor changes in, this region which is vulnerable to vision loss in glaucoma.

Ganglion Cells—Although the NFL is directly visible, the originating ganglion cells (GCs) have proven more elusive. Their relatively large size makes them resolvable, but they are weakly scattering (low SNR) and, in back reflected light, do not seem to possess the intrinsic contrast that might reveal their structure. Visualizing the GCs in living eyes has only been possible to date using extrinsic fluorophores. Using specially designed AOSLO systems, extrinsic fluorophores of various types have been employed to visualize ganglion cells in monkeys (G-CaMP3, (Yin et al 2014)), rats (eGFP, (Geng et al 2009)) and mice (G-CaMP3, (Yin et al 2013); YFP-expressing genetic strains for GCs (Geng et al 2012)). Two examples of GCs imaged in a YFP-expressing mouse are shown in Fig. 2. The images are especially well-resolved in part because the mouse has a higher numerical aperture then the human (see inset 1) which offers higher potential resolution (Geng et al 2011). In fact, the GC images shown here approach the resolution typically obtained of the same cell *in vitro*. Today, the use of fluorescent agents, other than sodium fluorescein, ICG and fluorescently-conjugated annexin V, is not permitted in human. Nevertheless, the ability to image these cells in mice has a major potential clinical impact as mice are the most common animal model for studying retinal disease.

Vasculature—A heathy vascular network is crucial to the health and function of the retina. The standard clinical method to visualize the vasculature in living human retina is to boost its contrast by recording fluorescence emission of sodium fluorescein or ICG injected systemically. Backscattered light in confocal AOSLO and AO fundus cameras has only had moderate success in visualizing the microvasculature (Martin & Roorda 2009, Popovic et al 2011).

Departures from conventional AO systems that detect backscattered light have proven most effective for all aspects of vascular imaging. An obvious first example is the combination of fluorescein angiography (FA) with AO. The combination of the high contrast of FA and high resolution of AO has yielded stunning images (Gray et al 2006, Pinhas et al 2013) (see Fig. 3A). But, as useful as sodium fluorescein is, FA is invasive, it generates its signal over a limited time course, and is not without side-effects.

The biggest advances in vascular imaging have emerged through the use of AOSLO detection schemes other than confocal (large pinhole, offset pinhole, dark field and split detector) and the use of motion contrast. These alternate detection schemes, which either block the direct back-scattered component (split-detector AOSLO or dark-field AOSLO) or are designed to admit more multiply scattered light (offset pinhole) can extract more signal from the actual blood flow as well as more details of the microvascular structure. Fig. 3B is

an image of an arteriole where purported mural cells composing the vessel wall are visualized.

With the ability to record AO-corrected videos of the retina another new source of contrast, motion contrast, emerged. In a video of the retina, scatter from most features remains relatively constant, but scattering and shadowing from blood cells generates a dynamic signal. By processing the videos to highlight only the dynamic element of the signal, exquisite vascular maps have been generated. Fig. 3C shows one example of a motion contrast perfusion image extracted from an AOSLO video acquired with a split detector (Sulai et al 2014). Incidentally, similar motion contrast approaches are emerging in OCT angiography as well.

Acquisition and registration of images that encode different aspects of structure and function are very effective for understanding complex systems (eg multiple fluorescent labels in microscopy). Similar benefits are beginning to be realized in for retinal imaging as well. Fig. 3D shows a fluorescent image of pericytes overlayed onto a motion contrast image of the retinal vasculature.

Bipolar Cells—To date, no AO system has reported on the visualization of bipolar cells. Like GCs, bipolar cells are resolvable but lack the scatter and intrinsic contrast to be readily seen by reflectance. Fluorescent labeling is the most likely approach by which these cells will be seen.

Henle Fibers—Moving deeper, there is a single report showing an image of purported Henle fibers, which are the elongated axons of cone and rod cells that connect to their tangentially displaced bipolar cells near the fovea. Like the NFL, the HFL is formed by array of highly oriented fibers which tend to exhibit strong orientation-dependent scattering characteristics (Lujan et al 2011). Under normal conditions, Henle's fibers do not run perpendicular to the imaging beam and are generally not seen. However, in the case of Best's Vitelliform disease shown in Fig. 4, the large subretinal lesion has distorted the inner retina, reorienting the fibers and giving rise to sufficient scatter to reveal their structure.

Photoreceptors—Photoreceptors were the first and have remained the most studied microscopic structure in the retina using AO. They are of direct interest, as they comprise the first neuron in the human visual system. It is important to note that, like the bipolar cells, the nuclei of the photoreceptors have not been resolved using AO system. Rather, it is the light scattered and emitted from the waveguiding portion of the cells (inner and outer segments). It is the waveguiding property of cones that gives them their excellent scattering properties and intrinsic contrast (Roorda & Williams 2002). Advances in ophthalmic AO technology over the years have led to significant improvements in our ability to image these cells, to the point where it is possible to record clear mosaics of rods and cones across much of the macular region. AO fundus cameras have had moderate success in imaging foveal cones and rods (Doble et al 2011), but confocal AOSLO has been the clear winner in this regard (Dubra et al 2011), as evidenced by the images in Fig. 5A.

While confocal AOSLO beats all modalities in terms of spatial resolution, the confocal aspect also limits the information that can be collected, sometimes giving a false impression of retinal structure (see Fig. 13). Two alternate approaches to image the photoreceptor array are shown in Figs. 5B&C. The first shows an image of the peripheral cone mosaic taken using split detector AOSLO (Scoles et al 2014b). The compromise to resolution inherent to the technique results in a failure to resolve the intervening rods (for comparison, see Fig. 5B), but the cones, or the inner segments of the cones, are unambiguous and take on an embossed appearance similar to *in vitro* microscope images using Nomarski optics (Curcio et al 1990). The fact that this technique does not rely on direct, backscattered light (which includes waveguided light) means that these structures might be visible, even when the cone is not waveguiding and scattering normally. This may prove useful in identifying whether or not photoreceptor inner segments remain after the outer segments, or other structural features that give rise to the waveguided photoreceptor reflection, are not present. In fact, such a case is reported in Fig. 13.

Finally, in the group in Rochester has managed to acquire images of the cone photoreceptor array in a macaque monkey using 2-photon fluorescence imaging of the intrinsic fluorophores in the photoreceptors (Hunter et al 2011). The implications of such an image are profound, as the 2-photon fluorescence signal indicates the presence of specific molecules in the retina. Resolved in this way, these signals may serve as effective biomarkers for retinal, or photoreceptor health. Recent results from that lab have shown significant improvements in efficiency and have expanded the scope of what can be visualized (Sharma et al 2013), but the approach is not yet ready for use in living human eyes.

Retinal Pigment Epithelium (RPE)—The RPE plays a crucial role for retinal health and function and is implicated as the primary affected cell in several diseases, most notably age-related macular degeneration. RPE cells are relatively large and fall easily within the resolution limits of the AOSLO system. OCT images also suggest that the RPE layer is a relatively strong back scatterer. However their visualization has proven difficult for AO fundus cameras and even confocal AOSLOs. The first reports of visible RPE cells were in selected cases of cone and rod degenerative diseases (Roorda et al 2007). The idea was that in a healthy retina the strong spatially resolved signal from the photoreceptors masked the relatively weaker scattering from the RPE, but when the photoreceptors were missing, the RPE was revealed. The presence of RPE and lack of photoreceptor cells was supported in that case by OCT images from the same locations.

Fig. 6A shows an example of an image of an RPE mosaic taken from a patient with retinitis pigmentosa. In confocal AOSLO, the mosaic is revealed because the scattered light comes from the vicinity of junctions between the cells, whereas the cell centers are hyporeflective. The source of scattered light is not known but coincides with lipofuscin accumulation (see Fig. 6B).

Fundus autofluorescence (FAF) is a technique that has been used to measure lipofuscin content in the retina, most prevalently in the RPE cells (Delori et al 1995). It was discovered that in an AOSLO system the same fluorescent signal could be used to resolve the RPE cells

(Morgan et al 2009). Fig. 6B shows an image of the RPE mosaic taken from the healthy human retina. Although the technique is less comfortable to the patient and carries the risk of potential phototoxicity (Hunter et al 2012, Morgan et al 2008), it offers a distinct advantage in that not only can the FAF signal be used to resolve cells, but also quantify their molecular content (in this case, the presence of lipofuscin).

Once again, the recent use of AOSLO detection schemes other than confocal, have proven effective to image cells not visible with confocal methods. By blocking the direct backscatter from the waveguiding photoreceptors and preferentially detecting multiply scattered light, Fig. 6C shows how dark-field AOSLO imaging can be used to record images of RPE mosaics in healthy human retinas (Scoles et al 2013). Corresponding confocal AOSLO images recorded simultaneously at the same location show the overlying photoreceptor mosaic.

Lamina Cribrosa (LC)—The final structures that benefit from AO imaging are in the region of the optic disk. In particular, AO has been used to reveal the microstructure of the LC, a porous network comprised of beams of flexible collagenous tissue forming the passageway for retinal vessels and nerve fibers in and out of the eye. Change in the LC structure from imbalance of pressure is suggested to contribute to ischemia and/or cause axonal damage to the nerve leading to glaucoma. Improved views of this structure, therefore, may reveal the mechanical changes that occur and their possible implications for optic nerve health. Fig. 7 shows an example LC image from a non-human primate retina (Ivers et al 2011). Although the AOSLO lacks the depth resolution and sensitivity of OCT methods to view the LC (for comparison see (Nadler et al 2014, Vienola et al 2012)), it generates the highest resolution images of the structure on the LC surface ever obtained. Significant changes have been found in LC structural parameters in non-human primates with experimental glaucoma (Sredar et al 2013, Vilupuru et al 2007) and in humans with glaucoma (Akagi et al 2012).

Subretinal Structures—The previous section covers the majority of structures in normal eyes that have been visualized using AO ophthalmoscopes. To date, no images of subretinal structures obtained with AO systems have been published, with the exception of some choroidal vascular details seen through geographic atrophy (which offers a window to the choroid and sclera). The main challenge to imaging subretinal structures is the weak signal arising from these layers. It is most likely that a combination of longer wavelengths and heterodyne detection (OCT), possibly combined with more innovative collection optics and AO will be the key to imaging subretinal structures at cellular level resolution.

3.2 Associating Function with Structure

The potential for AO imaging to offer new insight into eye disease and to accelerate efforts to treat eye disease is exciting, but it is important to understand that structural information only tells some of the story. An assessment of vision health is incomplete unless the functional consequences of the observed structure are understood. This section will highlight a number of ways in which AO has been used to make direct measures of functional

properties of retinal cells. It will be split into two sections; objective and subjective functional tests.

3.2.1 Objective Functional Tests—Cellular-level retinal photopigment densitometry using single acquired frames has been used to reveal important properties of cone photopigments (Hofer et al 2005a, Masella et al 2014a, Masella et al 2014b, Roorda & Williams 1999). The added dimension of time resolution in AO imaging though the use of video, first with AOSLO (Roorda et al 2002) and subsequently through a new generation of high-frame-rate AO fundus cameras (Bedggood & Metha 2013, Rha et al 2006), has broadened the scope of functional vision testing.

Encouraged by the discovery of significant light-induced optical scattering changes of photoreceptors found using an OCT system in an *in vitro* preparation (Bizheva et al 2006), several groups used AO to perform similar measures, but with the advantage of improved lateral resolution. It is important to note that with incoherent light, the source of detected signal change is due only to absorption of the tissue or changes in structure and/or refractive index giving rise to changes in scattered light magnitude whereas with coherent and partially coherent light, changes in detected light signal can also arise from interference. The latter signals can be very high contrast, masking the former. (Grieve & Roorda 2008) used low coherent light in a confocal AOSLO to look at average scattering changes over time using a 30 Hz AOSLO system and found changes on the order of 5% with multi-second time courses. Three groups have used partially coherent light and high speed AO fundus cameras to record fast changes in photoreceptor scattering in response to light stimulation. In all cases, significant fluctuations of the light from the photoreceptors were observed. When using partially coherent light (coherence lengths less than the twice the length of the outer segment) the source of the fluctuating signals is not well understood (Bedggood & Metha 2012b, Bedggood & Metha 2013, Rha et al 2006, Rha et al 2009). However, imaging with longer coherence lengths (greater than twice the OS length) a useful component of the interference signal that is directly related to the outer segment length can be recorded. Employing this signal, (Jonnal et al 2010) was able to measure the rate of growth of human cone outer segments. The combination of interferometry with AO was able to reliably measure an impressively slow rate of growth of 93-113 nm/hour!

Intrinsic signals from other, less reflective neurons in the retina have not, to date, been observed directly with AO systems. The only functional optical recording from inner retinal neurons using AO has relied on the use of a neural-activity-dependent fluorescent dyes (calcium indicators, G-CaMP3) in mice (Yin et al 2013) and in monkeys (Yin et al 2014). These fluorescent-based approaches are not yet ready for use in humans, but the accelerating development of effective viral-based cellular delivery systems for gene therapy and the possibility that these vectors may also be approved to carry fluorescent payloads means that these techniques may translate to human use sooner than we might have anticipated.

One of the most fruitful objective functional measures has been has been in the field of blood flow. Cellular access combined with high frame rate imaging has allowed for better characterization of hemodynamics than ever before. Fig. 8 includes a link to a short video from a high frame rate AO fundus camera in which individual red and white blood cells can

be tracked through the capillaries (Bedggood & Metha 2012a). In an AOSLO system, (Tam et al 2011b) used AOSLO videos to differentiate the different pathways that white and red blood cells prefer to take through the capillary network, identifying the 'leukocyte preferred paths'. Finally, (Zhong et al 2011) modified their AOSLO to switch between raster-scan and line scan mode. The raster scan mode was used to identify and target blood vessels. Once targeted, switching to line-scan model enabled extremely high-rate imaging of flow through the larger retinal vessels. The ability to measure functional properties of the micro-vasculature has implications that go beyond ophthalmic applications, possibly offering a new way to study more systemic disorders like Alzheimer's disease and diabetes. The use of AO to study vasculature in diabetes and other diseases is discussed in Sec 4.2.

A final objective functional measure is the ability to measure fixation stability and eye movements. Having a microscopic image of a living retina means that we can also know what direction the eye is pointing on the same scale. (Putnam et al 2005) used this to measure the locus of fixation in a human eye. With the advent of higher frame rate AO imaging, came the ability to measure fixational eye movements dynamically. In fact, an AOSLO can track motion at much higher rates than its frame rate, by analyzing the small distortions that are present within each acquired frame. Capitalizing on this property, analysis of AOSLO videos have generated the most accurate fixational eye motion statistics ever recorded (Stevenson & Roorda 2005).

The ability to measure eye movements might be useful to diagnose or better understand some eye diseases and neurological disorders. The ability to track and compensate for the eye's motion might also make it easier to image patients with abnormal eye movements, like nystagmus. Finally, the measurement of eye movement can facilitate functional testing at targeted locations (see Sec 3.2.2). However, routine eye tracking for the broader clinical population remains a challenge because of the small field size of typical AO systems combined with the relatively large movements associated with many eye diseases.

3.2.2 Subjective Functional Tests—AO systems can also be used to control the optical properties of light delivered to the retina. AO for vision correction was used early on to show expected improvements in contrast sensitivity (Liang et al 1997, Yoon & Williams 2002), but the correlations of structure and function are where the full technology was really demonstrated. (Hofer et al 2005b) used AO-corrected light delivery to study color percepts elicited by single cone stimulation. (Rossi & Roorda 2010) administered AO-corrected visual study the relationship between cone spacing and acuity at and near the fovea. Finally, (Makous et al 2006) used their AO system to test visibility of brief cone-sized flashes of light for a subject, who by all appearances in the AO retinal image, had an incomplete cone mosaic where about 1/3 of the cones were not visible, leaving visible gaps in the mosaic. They inferred from their results that these cone-sized gaps were indeed microscotomas.

As impressive as these early results were, the technology was only able to deliver AO-corrected stimuli, but was not able to target those stimuli to particular cells or specific retinal locations. Next, we describe a system that combines AO-imaging, eye-tracking and AO-corrected stimulus delivery to visualize, track and target individual cells with AO-corrected light stimuli. By performing the imaging and eye tracking in real time, (Arathorn et al 2007)

managed to achieve stimulus delivery accuracy of better than 1.3 microns. Further refinements to the processing (Yang et al 2010) and subsequent development of tools to measure and correct for transverse chromatic aberration (Harmening et al 2012), culminated in the ability to reliably perform vision testing experiments on single cone photoreceptors (Harmening et al 2014).

A system with this precise targeting capability holds promise for making important structure-function relationships in eye disease (Tuten et al 2012), where structural changes can be very focal. Sec 4.2 presents a specific example of the use of AO microperimetry for patients with macular telangiectasia type II.

4.0 How is AOSLO being used clinically?

4.1 Characterization of eye disease

The previous sections focused on the capabilities of today's AO systems. Over time, we can expect to see many of these new approaches translate to clinical applications. Nevertheless, AO is already having an impact in ophthalmology. The charts on Supplemental Information Figure 1 plot publication trends that indicate how AO is being used in ophthalmology today. There are three main trends that can be drawn from these charts: First, the total number of published papers continues to increase. Second, AOSLO systems are producing an increasing fraction of papers over time. Third, clinical applications are accounting for an increasing fraction of papers over time. Among the clinical papers, there are dozens which report on the use of AO imaging to better characterize a disease. These are valuable studies, especially the ones that report on a disease which is well-characterized clinically or genetically. Supplemental Information Table 1 shows a categorized list of ocular diseases with citations to all the relevant papers that have reported on them using AO systems.

4.2 New discoveries about eye disease

Characterization of eye disease is important and we can expect to see dozens of new papers in this field on numerous diseases. This section will focus on three particular eye diseases, diabetes, age-related macular degeneration (AMD), and macular telangiectasia, and expand on specifically how AO has been used to make entirely new discoveries or provide new insights about the mechanisms for the disease and its progression.

Diabetes and other vascular disease—Several AOSLO studies of diabetes have made new discoveries. In a cohort of patients with no diabetic retinopathy, (Tam et al 2011a) used confocal AOSLO with motion contrast to perform a series of high resolution structural and functional analyses of the retinal microvasculature near the fovea. In the patient cohort (diabetes without retinopathy), metrics including blood cell velocity, foveal avascular zone (FAZ) size and capillary density at the edges of the FAZ showed trends, but were no different from normal, possibly because the measurements are variable in a normal population and there were not enough subjects enrolled in each cohort to detect a difference. However one measurement - that of vessel tortuosity - *did* show a difference: capillaries around the FAZ in the diabetic patients were more tortuous. The hypothesis was that the less tortuous vessels, which serve as the leukocyte preferred paths and transport the majority of

white blood cells from arterioles to venules, were lost, leaving the more tortuous capillaries behind. This supposed vessel loss was too small to be detectable as FAZ enlargement or capillary density reduction, for reasons described above, but emerged from the tortuosity analysis. The loss of the leukocyte preferred paths was suggested to initiate a more rapid degeneration as leukocytes would have to find a new path from arterioles to veins through more tortuous, and consequently more vulnerable, paths.

In patients with mild to moderate non-proliferative diabetic retinopathy (Burns et al 2014) used offset pupil AOSLO and found significant vessel remodeling and revealed microvascular abnormalities with exquisite detail. Quantitatively, they found larger capillary diameters than normal (8.2 +/- 1.1 vs. 6.1 +/- 0.75 micrometers) around the foveal avascular zone. In arterioles, they found thicker vessels walls, and a significantly larger wall-to-lumen ratio between normal and diabetic retinas (1.1 +/- 0.87 vs. 0.42 +/- 0.28 micrometers).

Finally, (Dubow et al 2014) published a study using AOSLO fluorescein angiography to classify a rich and diverse array of microaneurysms in retinas affected by diabetes and other vascular diseases (see Fig. 9A). In one patient with a central retinal vein occlusion, they showed regression of a microaneurysm in response to VEGF treatment. A related paper reporting on the same patient presented 5 different ways the AO can visualize an individual microaneurysms (Chui et al 2014). Fig. 9B highlights two MAs that have quite a different appearance. These papers make an excellent case for AO imaging to better identify and classify vascular abnormalities and to track changes in these structures over time.

These highly sensitive measures, which would not have been possible without the resolution and contrast offered in AO systems, can indicate the earliest structural indications of disease and may provide useful biomarkers for disease progression or response to treatment.

Age-related Macular Degeneration (AMD)—AMD is a common eye disease and is a leading significant cause of vision loss among people age 50 and older (https://www.nei.nih.gov/eyedata/amd). Despite that fact that this disease is so prevalent and so extensively studied, the primary affected cells and the nature of the progression of the disease remain poorly understood (Lim et al 2012). Several recent AO studies shed light on this important disease and promise to accelerate efforts to understand and treat AMD. (Zayit-Soudry et al 2013) measured properties of cones over time in several AMD patients. Although they showed clear examples of cone disruption over some drusen and in areas of geographic atrophy, and the cone mosaics in AMD retinas often exhibited somewhat abnormal reflective characteristics, no progressive increase in cone spacing which might indicate a steady loss of cones was detected in a longitudinal study of the same regions over 12-21 months (compare with the progressive loss in cone density and increase in cone spacing for retinitis pigmentosa reported by (Talcott et al 2011)). This result suggests that cone loss is likely to occur consequent to other structural changes in AMD, like loss of RPE cells in geographic atrophy. Similarly, (Godara et al 2010) found undisrupted mosaics of cones over early drusen. These findings are supported by histology where the only disruptions in photoreceptors were seen over the drusen, but not in the areas adjacent to drusen (Johnson et al 2003). By comparison, AOSLO studies of cones over reticular pseudodrusen showed earlier and more prevalent loss of cone visibility (Meadway et al

2014, Zhang et al 2014), with normal appearing cones in the surrounding areas (see Fig. 10), perhaps due to direct damage to photoreceptors by subretinal drusenoid deposits beneath the photoreceptors, unlike typical drusen which exist beneath RPE cells that may sustain the overlying photoreceptors.

While photoreceptors may be suffering collateral damage from other changes in AMD, the RPE may undergo the earliest structural changes. Autofluorescence images collected with AOSLO shown in Fig. 11 find disruptions in the uniformity of the RPE layer in AMD patients (Rossi et al 2013).

Finally, an AO fundus camera was used to visualize and track clumps of melanin granules in the vicinity of geographic atrophy in patients with age-related macular degeneration (single frame shown on Fig. 12). They observed, for the first time, a dramatic movement of these granules over time, suggesting a potential important role of melanin in the progression of GA and identifying a possible biomarker for disease progression.

Macular Telangiectasia—Macular telangiectasia type 2 (Yannuzzi et al 2006) is less prevalent than diabetes or AMD, but a recent paper using a combination of AOSLO imaging and AO microperimetry highlights two discoveries that might prove to be relevant to many retinal degenerative diseases (Wang et al 2015). Patients with macular telangiectasia can present, at the early stages, with small discrete lesions in the photoreceptor layer close to fixation. Outside of these lesions, cones appear relatively normal. When Wang et al tracked these lesions over time, they found that although the overall size of the lesion expanded, some areas of the lesion showed a recovery of normally reflecting cones. Cone spacing measurements indicated that these recovered cones had normal spacing. It is unlikely that new cones were generated, so the most likely explanation was that these cones were present throughout the study, but were lacking the physical structure that gave rise to a visible reflection. To investigate further, the group used AO microperimetry to measure visual function of the recovered cones as well as at targeted locations across the lesion. They found normal sensitivity in the recovered cones, and measureable function, albeit reduced, in parts of the lesion that appeared, both by OCT and by confocal AOSLO, to be devoid of cones. There have been reports of the recovery of the IS/OS reflection in some diseases using OCT and recovery of cones in AOSLO (Ooto et al 2012, Ooto et al 2011), but this is the first time a clear and unambiguous array of cones has been shown to recover both functionally and structurally. It is also the first definitive measure of visual function in a region where AO imaging would have otherwise suggested a complete lack of cones.

This study reinforces the notion that one has to be cautious about inferring function directly from structure. It also highlights the needs for new imaging methods to reveal the structure. For example, split detector AOSLO imaging was not available for this study, but had it been used, it might have found a complete mosaic of inner segments in the part of the lesion that retained visual function as well as the part of the lesion that recovered normal reflectivity.

The study lends support to the idea that recoverable cones might exhibit a characteristic appearance with OCT (Chhablani et al 2012, Landa et al 2012). The specific characteristic is the preservation of the external limiting membrane above relatively transparent (dark) tissue

in the region where reflections consistent with the IS/OS and posterior tips of the outer segments are normally seen.

4.3 AO as a tool for clinical trials

Perhaps the most immediate benefit of AO will be in evaluating new treatments to cure, prevent or slow progression of eye disease. The ability of an AO ophthalmoscope to resolve cells and return to the same cells day after day offers the ability to track disease progression on an unprecedented cellular scale. Measuring progression of disease on this scale has normally only been possible in animal models and only then by sacrificing the animals with and without treatment at various stages of progression. AO offers two advantages: First, the microscopic imaging can be done in humans noninvasively. Second, imaging the same cells in the same human eye longitudinally reduces noise caused by differences in treatment response between individual patients, possibly making clinical trials more efficient and conclusive.

To date, the only published report in which AO images of photoreceptors were used to evaluate disease progression and response to an experimental treatment for retinal degeneration was by (Talcott et al 2011), in which they evaluated the efficacy of ciliary neurotrophic factor (CNTF) treatment for patients with retinitis pigmentosa. In a subset of 3 participants from a larger, multicenter Phase 2 clinical trial where one eye was treated with CNTF and the fellow eye served as a control, a significant difference was found - the cone density declined less rapidly in the treated eye over 24-32 months. While there is much more involved in assessing whether a treatment is working than simply monitoring the preservation of visible cones, AO technology offers the potential to make the path of drug development for eye disease faster and more cost effective. Currently, quantitative measures from AO images are being employed for use as primary and adjunct outcomes in three known clinical trials involving a treatment. First, a larger trial studying cone photoreceptor spacing in 30 patients with retinal degenerations as the primary outcome measure in response to CNTF treatment is currently enrolling patients (www.clinicaltrials.gov NCT01530659). A similar CNTF trial is underway for the treatment of macular telangiectasia type 2 (www.clinicaltrials.gov NCT01949324). Longitudinal measures of cone spacing and cone coverage are being collected in an ancillary study within this trial. Finally, photoreceptor survival as assessed from AO images will also be used to provide a secondary outcome in a Pfizer-sponsored stem cell therapy trial for AMD at University College London (www.clinicaltrials.gov NCT01691261).

4.4 Prescreening for suitable patients

This is an exciting time in the battle to treat and cure retinal degenerative disease. Gene therapy trials (Bainbridge et al 2008, Hauswirth et al 2008, Maguire et al 2008), retinal prosthetics (Weiland et al 2011), and stem cell therapies (Schwartz et al 2012, Schwartz et al 2015) are all showing promising results. And, thanks to the NEI Audacious Goals Initiative to “Regenerate Neurons and Neural Connections in the Eye and Visual System” (http://www.nei.nih.gov/audacious/), the notion of being able to offer solutions to patients with previously untreatable diseases is now more likely than ever. However, it will be especially important in the early stages of this effort to carefully identify the diseases that are amenable

to treatment, and equally important to identify patients who are at a stage of progression that is most amenable to treatment. It is likely that microscopic AO imaging will play an important role in screening these patients who are most likely to benefit.

Achromatopsia is the best example of this. Achromatopsia is a rare condition, affecting 1 in 30,000, but it is particularly relevant as it is slated for gene therapy trials in the near future (http://www.achromacorp.org/PathToCure.html). It is present at birth or early infancy and its symptoms include reduced acuity, photophobia, complete lack of or reduced color vision, and nystagmus. ERG measurements show a loss of cone function, but normal rod function. Mutations in the *CNGA3* and *CNGB3* gene, which encode the aspects of the cone phototransduction, account for about 70% of achromatopsia cases (Kohl et al 2005).

Although the gene is known, the prospects of genetic therapy benefiting this condition depend on the state of the retina. If a cone is present but dysfunctional, the prognosis is much better than if the cone has degenerated completely. In fact, OCT studies have shown that achromatopsia patients suffer varying degrees of degeneration. (Sundaram et al 2014) suggested that cones are indeed present in some cases but not in others. The first AO studies of this disease showed a marked lack of reflection in the regions where cones would normally reside, leaving holes in the mosaic (Genead et al 2011). More recently, the use of split-detector AOSLO imaging revealed mosaics of intact inner segments in the regions where confocal AOSLO images were hyporeflective in the same locations (see Fig. 13). This very specific finding is the perhaps the best indication for recoverable cones(Dubis et al 2014), in which restoration of the non-mutated gene to these cells stands a good chance to restore their complete structure and function.

4.5 Early diagnosis

Dozens of published reports on AO ophthalmoscopy tout early detection and diagnosis of eye disease as one of the key benefits of the technology, yet there remain no published reports where such an early detection or diagnosis has been made. This is not surprising, given that AO ophthalmoscopy is an emerging technology and that studies to validate the reliability and significance of the findings observed in AO images are ongoing. These new views of the retina require careful interpretation (see next section) and most ophthalmologists are unfamiliar with such views. Nevertheless, as known diseases continue to be characterized and new microscopic phenotypes continue to be discovered, AO imaging will be used to characterize their earliest stages. Moreover, with the massive growth in our understanding of the genetics of eye disease, it is just a matter of time before cohorts of subjects with well-known risk factors of eye disease will be studied and followed with AO imaging prior to any clinical symptoms and natural history studies of disease progression that include AO images will demonstrate the sensitivity and validity of this imaging technology. Finally, as treatments emerge, the importance of early diagnosis will become increasingly important.

5.0 Discussion

The results presented in this review aimed to show the promise of AO and associated applications for clinical applications. By all indications AO will become increasingly important in ophthalmology.

In terms of optical quality, the most recent results suggest that today's AO ophthalmoscopes - at least for normal eyes – have achieved the diffraction limit (Dubra et al 2011). Nevertheless, there is a lot of room for improvement in making these systems more robust for patients. Seemingly minor improvements such as improved fixation targets, better pupil and head alignment and simpler system operation will go a long way to reduce imaging times and make systems more useable by any ophthalmic technician. Hopefully, manufacturers of commercial AO systems will be able to help the field by tackling a lot of the ergonomic problems.

The real future technical advances in AO imaging, as so many of the selected examples in this review suggest, will be in how AO is used. OCT systems for example, which are not part of this review, can benefit tremendously from AO. Impressive work is already underway in several labs (Felberer et al 2014, Jonnal et al 2012, Zawadzki et al 2014, Zawadzki et al 2009).

5.1 Analysis and Interpretation

Perhaps the most important area where advances can be made is in the analysis and interpretation of retinal images. A careless or unprincipled interpretation of an AO image can lead to erroneous conclusions. Such conclusions will not only compromise our collective understanding of a disease, but they will diminish the perceived value of AO technology. A proper analysis and interpretation begins with a strong understanding of the imaging system and how it interacts with the retina. In the final sections of the discussion we offer a systematic approach to understanding and interpreting AO ophthalmoscope images.

Understand the imaging modality—Every imaging modality is designed to record a specific type of signal. Failing to understand the implications of this can lead to erroneous interpretations. Fig. 14 shows a striking example of differences between two modalities in how images of melanin pigment appear. In a color fundus photograph, melanin clumps appear dark and brownish. In OCT, they are hyperreflective. Similar hyperreflectivity is seen in AOSLO images in near infra-red light. However, a near infra-red (NIR) AO fundus camera sees the melanin pigment as dark. The hyperreflectivity of melanin granules is what makes them appear bright in OCT and NIR AOSLO, but in a full field AO fundus camera, this reflectivity seems to be offset by an even greater reflectivity integrated from all depths of the surrounding retinal structure, giving the same granules negative contrast.

A deep understanding of the imaging modality can lead to innovative adaptations of it. Confocal AOSLO for example, is effective at detecting direct back-scattered light from the plane of focus. So, conversely, offsetting the confocal pinhole, enlarging the confocal pinhole, or selectively blocking the confocal light and detecting the light outside of the confocal aperture can preferentially detect multiply scattered light. The exquisite control of

the optics offered by AO allows for equally precise control of the how the light is detected. As such, alternate AOSLO detection schemes such as offset pinhole AOSLO (Chui et al 2012), dark field AOSLO (Scoles et al 2013) and split-detector AOSLO (Scoles et al 2014b) are poised to have a major impact on the field.

Understand the optical role of the retina and how it interacts with the imaging modality—The retina is comprised of a diversity of optically active structures. Absorption and scattering by the blood vessels, for example, cast shadows into the deeper retinal layers especially when using short wavelength light (see Fig 6(B) for an example). The characteristic structure of the vasculature make it easy to identify them as shadows and not actual scattering changes in the deeper layers but, in the case of microaneurysms, this distinction may not be as obvious (Ooto et al 2013) unless one takes a multimodal approach as described in the next section.

The waveguiding cones are another example. Cones and rods are optical fibers whose axes typically point toward the center of the pupil. The small reflection from a healthy cone (maybe 1% at most) is efficiently guided back toward the pupil making it readily visible in a properly focused AO retinal image. However, if the cone is not aligned properly it will no longer be an efficient back-reflector. While this does not likely explain the variation in cone reflectivity seen in a typical AO image in normal eyes (Roorda & Williams 2002) it is likely one of the reasons why cones at the edge of drusen appear dark (see Fig. 10). Nevertheless, a failure to visualize a cone does not immediately imply a missing cone or even a lack of cone function (see Sec 4.2 or see (Wang et al 2015)). The reflection from a cone might be weak and the dynamic range of the camera might not be high enough to detect it, but the dynamic range of human light sensitivity can be very high (Rodieck 1998).

The regular arrangement of fibers in the nerve fiber layer (NFL) as well as Henle fiber layer (HFL) gives rise to strong backscatter for light that is normally incident to their surfaces. This property is what makes the NFL so visible in confocal AOSLO and OCT. The HFL has the same scattering properties, but is less visible since the fibers do not run tangential to the retinal surface. Fig. 4 shows that in cases when retinal pathology deforms these structures, they can become visible.

Most of the inner retinal cells (ganglion cells, Müller cells, bipolar cells, photoreceptor nuclei) are transparent by design and have not been seen directly with AO imaging. Here, phase-sensitive approaches, like split-detector AOSLO, which have already revealed otherwise transparent inner segments (see Figs. 5B & 13) might find some success for other transparent retinal cells.

Unlike the inner layers of the retina, the RPE and other subretinal structures are highly absorptive and multiply scattering. For these structures, confocal detection approaches are not generally suitable. The best images of deep retinal layers will come from systems that are more sensitive to weak signals (eg. OCT), use longer wavelengths like 1060 nm to reduce effects of multiple scattering and avoid absorption by melanin, preferentially detect a depolarization signal, or use non-confocal AOSLO detection.

With a better understanding of retinal optics (Putnam et al 2010) comes the opportunity to take advantage of them. For example, the cone photoreceptor contains two relatively discrete reflections from near the IS/OS junction and the cone outer segment tips (COST) (Jonnal et al 2014). When light of the proper coherence length is used, these two reflections become mutually coherent (an optical condition which allows them to constructively or destructively interfere with each other) forming, in effect, a local interferometer. (Jonnal et al 2010) capitalized on this feature to measure the rate of growth of outer segments.

Use multimodal imaging whenever possible—Given the limits of any single imaging modality's ability to reveal retinal structure or function, it is useful to integrate the results from multiple modalities whenever possible. This is especially important for new technologies, where there is often far less amassed experience in reading and interpretation of the images. In its simplest form, multimodal systems that integrate wide field fundus views for identifying and then targeting high resolution imaging to specific regions of interest are proving to be very useful in a clinical setting (Huang et al 2012). But the advantages go far beyond the obvious ergonomic benefits. The combination of OCT and AO ophthalmoscopes (SLO or AO fundus cameras) is an excellent example. Fig. 10 shows how two modalities combined reveal a unique phenotype associated with reticular pseudodrusen.

To make the best use of multimodal information, it is very important to accurately register the images from the different modalities. This is not a new idea; commercial systems like the Heidelberg Spectralis are an example of a system with excellent integration of SLO and SD-OCT. Similar efforts in today's AO research labs are showing the same value on a microscopic scale (Felberer et al 2014).

In microscopy, the use of specific fluorescent labels to co-localize targets within and between cells is commonly used and is extremely valuable. Analogous approaches are only beginning to be applied to ophthalmoscopy. Although the scale of colocalization in the retina is much coarser, the knowledge gained will be just as useful, and the colocalized measures can also be more diverse, incorporating structural, molecular and functional information. In this review, there are 6 examples of colocalization: Fig. 3D: pericytes and perfused capillaries; Fig 9: 4 different modes of AOSLO imaging (5 including the movie); Fig 10: AOSLO and OCT; Fig 13: Split-detector and confocal AOSLO; Fig 14: color fundus camera, fundus autofluorescence, confocal AOSLO, OCT and AO fundus camera.

It is safer to make conclusions about what can be seen in an image than about what cannot—As mentioned previously, all imaging modalities are limited in the phenomena that they record. This is both good and bad. Fluorescein angiography, for example, detects fluorescent light coming from dye injected into the bloodstream, thereby serving to enhance contrast. Also, confocal AOSLO is only sensitive to direct back-reflections from the plane of focus, enhancing contrast and subserving optical sectioning. These technologies, by design, do not detect other aspects of the signal. The fact that neither of these modalities visualizes the RPE cells does not mean that the RPE cells are absent. Dark-field AOSLO, by comparison, does not show photoreceptors but shows the RPE mosaic (see Fig. 6C or refer to (Scoles et al 2013)). None of the above-mentioned modalities, to date, has visualized ganglion cells, but no one would suggest that they are not

present. Perhaps the best example of something that is not seen is in achromatopsia, where ‘holes’ in the cone mosaic seen with confocal AOSLO are readily seen as a mosaic of inner segments using split-detector AOSLO imaging (see Fig. 13). For this reason, judicious use of multiple modalities to assess retinal structure and function will often help to make conclusions about the presence or absence of cells.

One example regards a seemingly simple measure of cone density, which is a measure of the number of cones per unit area. An accurate measurement of cone density requires that every single cone in the selected area be identified. If an obscuration within the inner retinal layers renders the underlying cones dark, then a decision to not consider these regions as containing potential cones will lead to a measurement artifact of reduced density. In patients with retinal disease, subtle disruptions of the inner retinal structure are common and can give rise to deep shadows in the retina layers. A more conservative approach might be to measure cone spacing, which is less prone to these artifacts if computed correctly (Duncan et al 2007).

Is this a bad image of a healthy retina, or a good image of a diseased retina?—This remains an unsolved problem in the field of AO imaging, even though AO ophthalmoscopes have access to more information that can bear on the quality of an image than any other imaging modality. The AO control loop generally aims to minimize the wavefront errors and continuously recorded metrics like the residual wavefront aberration error can potentially be used as an indication of the quality of the correction. But if there are remaining aberrations that are undetectable, such as those caused by tear film changes or cataract, the aberration correction might be far worse than the AO system is reporting. Also, the focus setting of an AO ophthalmoscope is generally decoupled from the AO control so even though the system might have a perfect AO correction, the image may be poor because it is improperly focused on the structures of interest.

The best approach to assessing the quality of the image ultimately has to reside in the image itself. Image quality metrics, like standard deviation or contrast will be useful (Larocca et al 2013, Sulai & Dubra 2014). In confocal AOSLO imaging, gauging the magnitude of light detected through the pinhole is a simple and effective strategy (Hofer et al 2011, Li et al 2009), although with some shortcomings (Sulai & Dubra 2014).

Use automated image analysis tools with caution—AO systems can collect a tremendous amount of data in a short period of time. For this reason, automated methods to generate and analyze images are sorely needed. Automated systems to assemble montages (stitching together a collection of AO images to for a larger image) are already being developed and used (Huang et al 2012), but the scope for automation goes far beyond that.

By far, the bulk of the automation effort in AO ophthalmoscopy has been focused on automatic identification of photoreceptors from AO images. Not only are the photoreceptors the most commonly imaged structures but photoreceptor metrics such as density, spacing and regularity have been used for decades to understand many aspects of vision, from acuity (Geller et al 1992, Hirsch & Curcio 1989) to degenerative eye disease (Milam et al 1998). Several cell counting algorithms have been developed and improved upon and these

algorithms are regularly used (Chiu et al 2013, Cooper et al 2013, Li & Roorda 2007, Xue et al 2007). By all indications, these algorithms are very effective in identifying cones in good images from normal eyes. However, the success of these algorithms should never be assumed to have concomitant success with diseased eyes. The fact is, aside from a few filters designed to avoid impossible events like finding cones that are too close together, these algorithms do little more than detect bright spots in an image. These algorithms are just as likely to detect 'cones' in a speckly image of the nerve fiber layer, or within the bright reflected light from an area of geographic atrophy, as they are to find actual cones.

Therefore, today's automated approaches to identify cones should be used with caution, if at all, for studying patients. If today's algorithms are used, then it is advised to employ a multimodal approach and provide additional evidence that cones are present (for example, by confirming that the reflections associated with cones are seen in the same region with OCT)

6.0 Conclusions

Over the past 25 years, we have witnessed tremendous advances in the field of ophthalmoscopy, and this review provides a snapshot of the part that AO has played over this period. History reminds us that we cannot anticipate the developments that will take place in the future, and so it is risky to predict exactly how AO will be employed in ophthalmoscopy, even in the next decade. But AO is not a stand-alone technology – it is a general approach that offers microscopic optical access to the retina of a living eye. So, like other enabling technologies (digital cameras, light sources, faster signal processing), AO will certainly continue to play a role in future developments in ophthalmoscopy in our lifetimes.

Supplementary Material

Refer to Web version on PubMed Central for supplementary material.

References

Akagi T, Hangai M, Takayama K, Nonaka A, Ooto S, Yoshimura N. In vivo imaging of lamina cribrosa pores by adaptive optics scanning laser ophthalmoscopy. Invest Ophthalmol Vis Sci. 2012; 53:4111–19. [PubMed: 22669726]

Arathorn DW, Yang Q, Vogel CR, Zhang Y, Tiruveedhula P, Roorda A. Retinally Stabilized Cone-Targeted Stimulus Delivery. Optics Express. 2007; 15:13731–44. [PubMed: 19550644]

Bainbridge JW, Smith AJ, Barker SS, Robbie S, Henderson R, et al. Effect of gene therapy on visual function in Leber's congenital amaurosis. N Engl J Med. 2008; 358:2231–39. [PubMed: 18441371]

Bedggood P, Metha A. Direct visualization and characterization of erythrocyte flow in human retinal capillaries. Biomed Opt Express. 2012a; 3:3264–77. [PubMed: 23243576]

Bedggood P, Metha A. Variability in bleach kinetics and amount of photopigment between individual foveal cones. Invest Ophthalmol Vis Sci. 2012b; 53:3673–81. [PubMed: 22531694]

Bedggood P, Metha A. Optical imaging of human cone photoreceptors directly following the capture of light. PLoS One. 2013; 8:e79251. [PubMed: 24260177]

Bizheva K, Pflug R, Hermann B, Povazay B, Sattmann H, et al. Optophysiology: depth-resolved probing of retinal physiology with functional ultrahigh-resolution optical coherence tomography. Proc Natl Acad Sci USA. 2006; 103:5066–71. [PubMed: 16551749]

Burns SA, Elsner AE, Chui TY, Vannasdale DA Jr, Clark CA, et al. In vivo adaptive optics microvascular imaging in diabetic patients without clinically severe diabetic retinopathy. Biomed Opt Express. 2014; 5:961–74. [PubMed: 24688827]

Chhablani JK, Kim JS, Cheng L, Kozak I, Freeman W. External limiting membrane as a predictor of visual improvement in diabetic macular edema after pars plana vitrectomy. Graefe's archive for clinical and experimental ophthalmology = Albrecht von Graefes Archiv fur klinische und experimentelle Ophthalmologie. 2012; 250:1415–20.

Chiu SJ, Lokhnygina Y, Dubis AM, Dubra A, Carroll J, et al. Automatic cone photoreceptor segmentation using graph theory and dynamic programming. Biomed Opt Express. 2013; 4:924–37. [PubMed: 23761854]

Chui TY, Dubow M, Pinhas A, Shah N, Gan A, et al. Comparison of adaptive optics scanning light ophthalmoscopic fluorescein angiography and offset pinhole imaging. Biomed Opt Express. 2014; 5:1173–89. [PubMed: 24761299]

Chui TY, Gast TJ, Burns SA. Imaging of vascular wall fine structure in the human retina using adaptive optics scanning laser ophthalmoscopy. Invest Ophthalmol Vis Sci. 2013; 54:7115–24. [PubMed: 24071955]

Chui TY, Vannasdale DA, Burns SA. The use of forward scatter to improve retinal vascular imaging with an adaptive optics scanning laser ophthalmoscope. Biomed Opt Express. 2012; 3:2537–49. [PubMed: 23082294]

Cooper RF, Dubis AM, Pavaskar A, Rha J, Dubra A, Carroll J. Spatial and temporal variation of rod photoreceptor reflectance in the human retina. Biomed Opt Express. 2011; 2:2577–89. [PubMed: 21991550]

Cooper RF, Langlo CS, Dubra A, Carroll J. Automatic detection of modal spacing (Yellott's ring) in adaptive optics scanning light ophthalmoscope images. Ophthalmic Physiol Opt. 2013; 33:540–49. [PubMed: 23668233]

Curcio CA, Sloan KR, Kalina RE, Hendrickson AE. Human photoreceptor topography. Journal of Comparitive Neurology. 1990; 292:497–523.

Delori FC, Dorey CK, Staurenghi G, Arend O, Goger DG, Weiter JJ. In vivo fluorescence of the ocular fundus exhibits retinal pigment epithelium lipofuscin characteristics. Invest Ophthalmol Vis Sci. 1995; 36:718–29. [PubMed: 7890502]

Doble N, Choi SS, Codona JL, Christou J, Enoch JM, Williams DR. In vivo imaging of the human rod photoreceptor mosaic. Opt Lett. 2011; 36:31–33. [PubMed: 21209677]

Dubis AM, Cooper RF, Aboshiha J, Langlo CS, Sundaram V, et al. Genotype-dependent variability in residual cone structure in achromatopsia: toward developing metrics for assessing cone health. Invest Ophthalmol Vis Sci. 2014; 55:7303–11. [PubMed: 25277229]

Dubow M, Pinhas A, Shah N, Cooper RF, Gan A, et al. Classification of human retinal microaneurysms using adaptive optics scanning light ophthalmoscope fluorescein angiography. Invest Ophthalmol Vis Sci. 2014; 55:1299–309. [PubMed: 24425852]

Dubra A, Sulai Y. Reflective afocal broadband adaptive optics scanning ophthalmoscope. Biomed Opt Express. 2011; 2:1757–68. [PubMed: 21698035]

Dubra A, Sulai Y, Norris JL, Cooper RF, Dubis AM, et al. Noninvasive imaging of the human rod photoreceptor mosaic using a confocal adaptive optics scanning ophthalmoscope. Biomed Opt Express. 2011; 2:1864–76. [PubMed: 21750765]

Duncan JL, Zhang Y, Gandhi J, Nakanishi C, Othman M, et al. High-resolution imaging with adaptive optics in patients with inherited retinal degeneration. Invest Ophthalmol Vis Sci. 2007; 48:3283–91. [PubMed: 17591900]

Felberer F, Kroisamer JS, Baumann B, Zotter S, Schmidt-Erfurth U, et al. Adaptive optics SLO/OCT for 3D imaging of human photoreceptors in vivo. Biomed Opt Express. 2014; 5:439–56. [PubMed: 24575339]

Fernandez EJ, Prieto PM, Artal P. Binocular adaptive optics visual simulator. Opt Lett. 2009; 34:2628–30. [PubMed: 19724513]

Geller AM, Sieving PA, Green DG. Effect on grating identification of sampling with degenerate arrays. Journal of the Optical Society of America A. 1992; 9:472–77.

Genead MA, Fishman GA, Rha J, Dubis AM, Bonci DM, et al. Photoreceptor structure and function in patients with congenital achromatopsia. Invest Ophthalmol Vis Sci. 2011; 52:7298–308. [PubMed: 21778272]

Geng Y, Dubra A, Yin L, Merigan WH, Sharma R, et al. Adaptive optics retinal imaging in the living mouse eye. Biomed Opt Express. 2012; 3:715–34. [PubMed: 22574260]

Geng Y, Greenberg KP, Wolfe R, Gray DC, Hunter JJ, et al. In vivo imaging of microscopic structures in the rat retina. Invest Ophthalmol Vis Sci. 2009; 50:5872–79. [PubMed: 19578019]

Geng Y, Schery LA, Sharma R, Dubra A, Ahmad K, et al. Optical properties of the mouse eye. Biomed Opt Express. 2011; 2:717–38. [PubMed: 21483598]

Gocho K, Sarda V, Falah S, Sahel JA, Sennlaub F, et al. Adaptive optics imaging of geographic atrophy. Invest Ophthalmol Vis Sci. 2013; 54:3673–80. [PubMed: 23620431]

Godara P, Siebe C, Rha J, Michaelides M, Carroll J. Assessing the photoreceptor mosaic over drusen using adaptive optics and SD-OCT. Ophthalmic Surg Lasers Imaging. 2010; 41(Suppl):S104–S08. [PubMed: 21117594]

Gray DC, Merigan W, Wolfing JI, Gee BP, Porter J, et al. In vivo fluorescence imaging of primate retinal ganglion cells and retinal pigment epithelium cells. Optics Express. 2006; 14:7144–58. [PubMed: 19529085]

Grieve K, Roorda A. Intrinsic signals from human cone photoreceptors. Invest Ophthalmol Vis Sci. 2008; 49:713–19. [PubMed: 18235019]

Guo H, Atchison DA, Birt BJ. Changes in through-focus spatial visual performance with adaptive optics correction of monochromatic aberrations. Vision Res. 2008; 48:1804–11. [PubMed: 18597809]

Harmening WM, Tiruveedhula P, Roorda A, Sincich LC. Measurement and correction of transverse chromatic offsets for multi-wavelength retinal microscopy in the living eye. Biomed Opt Express. 2012; 3:2066–77. [PubMed: 23024901]

Harmening WM, Tuten WS, Roorda A, Sincich LC. Mapping the perceptual grain of the human retina. J Neurosci. 2014; 34:5667–77. [PubMed: 24741057]

Hauswirth WW, Aleman TS, Kaushal S, Cideciyan AV, Schwartz SB, et al. Treatment of leber congenital amaurosis due to RPE65 mutations by ocular subretinal injection of adeno-associated virus gene vector: short-term results of a phase I trial. Hum Gene Ther. 2008; 19:979–90. [PubMed: 18774912]

Hirsch J, Curcio CA. The spatial resolution capacity of human foveal retina. Vision Res. 1989; 29:1095–101. [PubMed: 2617858]

Hofer H, Carroll J, Neitz J, Neitz M, Williams DR. Organization of the human trichromatic cone mosaic. J Neurosci. 2005a; 25:9669–79. [PubMed: 16237171]

Hofer H, Singer B, Williams DR. Different sensations from cones with the same pigment. Journal of Vision. 2005b; 5:444–54. [PubMed: 16097875]

Hofer H, Sredar N, Queener H, Li C, Porter J. Wavefront sensorless adaptive optics ophthalmoscopy in the human eye. Opt Express. 2011; 19:14160–71. [PubMed: 21934779]

Huang G, Gast TJ, Burns SA. In vivo adaptive optics imaging of the temporal raphe and its relationship to the optic disc and fovea in the human retina. Invest Ophthalmol Vis Sci. 2014; 55:5952–61. [PubMed: 25146991]

Huang G, Qi X, Chui TY, Zhong Z, Burns SA. A clinical planning module for adaptive optics SLO imaging. Optometry and Vision Science. 2012; 89:593–601. [PubMed: 22488269]

Hunter JJ, Masella B, Dubra A, Sharma R, Yin L, et al. Images of photoreceptors in living primate eyes using adaptive optics two-photon ophthalmoscopy. Biomed Opt Express. 2011; 2:139–48. [PubMed: 21326644]

Hunter JJ, Morgan JI, Merigan WH, Sliney DH, Sparrow JR, Williams DR. The susceptibility of the retina to photochemical damage from visible light. Prog Retin Eye Res. 2012; 31:28–42. [PubMed: 22085795]

Ivers KM, Li C, Patel N, Sredar N, Luo X, et al. Reproducibility of measuring lamina cribrosa pore geometry in human and nonhuman primates with in vivo adaptive optics imaging. Invest Ophthalmol Vis Sci. 2011; 52:5473–80. [PubMed: 21546533]

Johnson PT, Lewis GP, Talaga KC, Brown MN, Kappel PJ, et al. Drusen-associated degeneration in the retina. Invest Ophthalmol Vis Sci. 2003; 44:4481–88. [PubMed: 14507896]

Jonnal RS, Besecker JR, Derby JC, Kocaoglu OP, Cense B, et al. Imaging outer segment renewal in living human cone photoreceptors. Opt Express. 2010; 18:5257–70. [PubMed: 20389538]

Jonnal RS, Kocaoglu OP, Wang Q, Lee S, Miller DT. Phase-sensitive imaging of the outer retina using optical coherence tomography and adaptive optics. Biomed Opt Express. 2012; 3:104–24. [PubMed: 22254172]

Jonnal RS, Kocaoglu OP, Zawadzki RJ, Lee SH, Werner JS, Miller DT. The cellular origins of the outer retinal bands in optical coherence tomography images. Invest Ophthalmol Vis Sci. 2014; 55:7904–18. [PubMed: 25324288]

Kohl S, Varsanyi B, Antunes GA, Baumann B, Hoyng CB, et al. CNGB3 mutations account for 50% of all cases with autosomal recessive achromatopsia. Eur J Hum Genet. 2005; 13:302–08. [PubMed: 15657609]

Landa G, Gentile RC, Garcia PM, Muldoon TO, Rosen RB. External limiting membrane and visual outcome in macular hole repair: spectral domain OCT analysis. Eye (Lond). 2012; 26:61–9. [PubMed: 21979863]

Larocca F, Dhalla AH, Kelly MP, Farsiu S, Izatt JA. Optimization of confocal scanning laser ophthalmoscope design. J Biomed Opt. 2013; 18:076015. [PubMed: 23864013]

Li KY, Mishra S, Tiruveedhula P, Roorda A. Comparison of Control Algorithms for a MEMS-based Adaptive Optics Scanning Laser Ophthalmoscope. Proc Am Control Conf. 2009; 2009:3848–53. [PubMed: 20454552]

Li KY, Roorda A. Automated identification of cone photoreceptors in adaptive optics retinal images. J Opt Soc Am A Opt Image Sci Vis. 2007; 24:1358–63. [PubMed: 17429481]

Liang J, Grimm B, Goelz S, Bille JF. Objective measurement of wave aberrations of the human eye with use of a Hartmann-Shack wave-front sensor. Journal of the Optical Society of America A. 1994; 11:1949–57.

Liang J, Williams DR. Aberrations and retinal image quality of the normal human eye. Journal of the Optical Society of America A. 1997; 14:2873–83.

Liang J, Williams DR, Miller D. Supernormal vision and high-resolution retinal imaging through adaptive optics. Journal of the Optical Society of America A. 1997; 14:2884–92.

Lim LS, Mitchell P, Seddon JM, Holz FG, Wong TY. Age-related macular degeneration. Lancet. 2012; 379:1728–38. [PubMed: 22559899]

Lujan BJ, Roorda A, Knighton RW, Carroll J. Revealing Henle's Fiber Layer Using Spectral Domain Optical Coherence Tomography. Invest Ophthalmol Vis Sci. 2011; 52:1486–92. [PubMed: 21071737]

Maguire AM, Simonelli F, Pierce EA, Pugh EN Jr, Mingozzi F, et al. Safety and efficacy of gene transfer for Leber's congenital amaurosis. N Engl J Med. 2008; 358:2240–48. [PubMed: 18441370]

Makous W, Carroll J, Wolfing JI, Lin J, Christie N, Williams DR. Retinal microscotomas revealed with adaptive-optics microflashes. Invest Ophthalmol Vis Sci. 2006; 47:4160–67. [PubMed: 16936137]

Martin JA, Roorda A. Pulsatility of parafoveal capillary leukocytes. Experimental Eye Research. 2009; 88:356–60. [PubMed: 18708051]

Masella BD, Hunter JJ, Williams DR. New wrinkles in retinal densitometry. Invest Ophthalmol Vis Sci. 2014a; 55:7525–34. [PubMed: 25316726]

Masella BD, Hunter JJ, Williams DR. Rod photopigment kinetics after photodisruption of the retinal pigment epithelium. Invest Ophthalmol Vis Sci. 2014b; 55:7535–44. [PubMed: 25316724]

Meadway A, Wang X, Curcio CA, Zhang Y. Microstructure of subretinal drusenoid deposits revealed by adaptive optics imaging. Biomed Opt Express. 2014; 5:713–27. [PubMed: 24688808]

Milam AH, Li ZY, Fariss RN. Histopathology of the human retina in retinitis pigmentosa. Progress in Retinal and Eye Research. 1998; 17:175–205. [PubMed: 9695792]

Miller, DT.; Roorda, A. Adaptive Optics in Retinal Microscopy and Vision. In: Bass, M., editor. Handbook of Optics. Vol. III. Rochester: Optical Society of America; 2009.

Morgan JI, Dubra A, Wolfe R, Merigan WH, Williams DR. In vivo autofluorescence imaging of the human and macaque retinal pigment epithelial cell mosaic. Invest Ophthalmol Vis Sci. 2009; 50:1350–59. [PubMed: 18952914]

Morgan JI, Hunter JJ, Masella B, Wolfe R, Gray DC, et al. Light-induced retinal changes observed with high-resolution autofluorescence imaging of the retinal pigment epithelium. Invest Ophthalmol Vis Sci. 2008; 49:3715–29. [PubMed: 18408191]

Nadler Z, Wang B, Schuman JS, Ferguson RD, Patel A, et al. In vivo three-dimensional characterization of the healthy human lamina cribrosa with adaptive optics spectral-domain optical coherence tomography. Invest Ophthalmol Vis Sci. 2014; 55:6459–66. [PubMed: 25228539]

Ooto S, Hangai M, Takayama K, Ueda-Arakawa N, Hanebuchi M, Yoshimura N. Photoreceptor damage and foveal sensitivity in surgically closed macular holes: an adaptive optics scanning laser ophthalmoscopy study. American Journal of Ophthalmology. 2012; 154:174–86. [PubMed: 22534108]

Ooto S, Hangai M, Takayama K, Ueda-Arakawa N, Tsujikawa A, et al. Comparison of cone pathologic changes in idiopathic macular telangiectasia types 1 and 2 using adaptive optics scanning laser ophthalmoscopy. American Journal of Ophthalmology. 2013; 155:1045–57. [PubMed: 23465268]

Ooto S, Hangai M, Yoshimura N. Photoreceptor restoration in unilateral acute idiopathic maculopathy on adaptive optics scanning laser ophthalmoscopy. Archives of Ophthalmology. 2011; 129:1633–35. [PubMed: 22159690]

Pinhas A, Dubow M, Shah N, Chui TY, Scoles D, et al. In vivo imaging of human retinal microvasculature using adaptive optics scanning light ophthalmoscope fluorescein angiography. Biomed Opt Express. 2013; 4:1305–17. [PubMed: 24009994]

Popovic Z, Knutsson P, Thaung J, Owner-Petersen M, Sjostrand J. Noninvasive imaging of human foveal capillary network using dual-conjugate adaptive optics. Invest Ophthalmol Vis Sci. 2011; 52:2649–55. [PubMed: 21228372]

Porter, J. Adaptive Optics for Vision Science. Hoboken, NJ: Wiley-Interscience; 2006.

Putnam NM, Hammer DX, Zhang Y, Merino D, Roorda A. Modeling the foveal cone mosaic imaged with adaptive optics scanning laser ophthalmoscopy. Opt Express. 2010; 18:24902–16. [PubMed: 21164835]

Putnam NM, Hofer H, Doble N, Chen L, Carroll J, Williams DR. The locus of fixation and the foveal cone mosaic. Journal of Vision. 2005; 5:632–39. [PubMed: 16231998]

Ramaswamy G, Lombardo M, Devaney N. Registration of adaptive optics corrected retinal nerve fiber layer (RNFL) images. Biomed Opt Express. 2014; 5:1941–51. [PubMed: 24940551]

Rha J, Jonnal RS, Thorn KE, Qu J, Zhang Y, Miller DT. Adaptive optics flood-illumination camera for high speed retinal imaging. Opt Express. 2006; 14:4552–69. [PubMed: 19516608]

Rha J, Schroeder B, Godara P, Carroll J. Variable optical activation of human cone photoreceptors visualized using a short coherence light source. Opt Lett. 2009; 34:3782–84. [PubMed: 20016612]

Rodieck, RW. The First Steps in Seeing. Sunderland, MA: Sinauer Associates; 1998.

Roorda A. Adaptive optics for studying visual function: a comprehensive review. J Vis. 2011; 11:1–21.

Roorda A, Romero-Borja F, Donnelly WJ, Queener H, Hebert TJ, Campbell MCW. Adaptive optics scanning laser ophthalmoscopy. Optics Express. 2002; 10:405–12. [PubMed: 19436374]

Roorda A, Williams DR. The arrangement of the three cone classes in the living human eye. Nature. 1999; 397:520–22. [PubMed: 10028967]

Roorda A, Williams DR. Optical fiber properties of individual human cones. Journal of Vision. 2002; 2:404–12. [PubMed: 12678654]

Roorda A, Zhang Y, Duncan JL. High-resolution in vivo imaging of the RPE mosaic in eyes with retinal disease. Invest Ophthalmol Vis Sci. 2007; 48:2297–303. [PubMed: 17460294]

Rossi EA, Rangel-Fonseca P, Parkins K, Fischer W, Latchney LR, et al. In vivo imaging of retinal pigment epithelium cells in age related macular degeneration. Biomed Opt Express. 2013; 4:2527–39. [PubMed: 24298413]

Rossi EA, Roorda A. The relationship between visual resolution and cone spacing in the human fovea. Nat Neurosci. 2010; 13:156–57. [PubMed: 20023654]

Sawides L, Gambra E, Pascual D, Dorronsoro C, Marcos S. Visual performance with real-life tasks under adaptive-optics ocular aberration correction. J Vis. 2010; 10:19. [PubMed: 20616133]

Schallek J, Geng Y, Nguyen H, Williams DR. Morphology and topography of retinal pericytes in the living mouse retina using in vivo adaptive optics imaging and ex vivo characterization. Invest Ophthalmol Vis Sci. 2013; 54:8237–50. [PubMed: 24150762]

Schwartz SD, Hubschman JP, Heilwell G, Franco-Cardenas V, Pan CK, et al. Embryonic stem cell trials for macular degeneration: a preliminary report. Lancet. 2012; 379:713–20. [PubMed: 22281388]

Schwartz SD, Regillo CD, Lam BL, Eliott D, Rosenfeld PJ, et al. Human embryonic stem cell-derived retinal pigment epithelium in patients with age-related macular degeneration and Stargardt's macular dystrophy: follow-up of two open-label phase 1/2 studies. Lancet. 2015; 385:509–16. [PubMed: 25458728]

Schwarz C, Manzanera S, Artal P. Binocular visual performance with aberration correction as a function of light level. J Vis. 2014; 14:6. [PubMed: 25515764]

Scoles D, Higgins BP, Cooper RF, Dubis AM, Summerfelt P, et al. Microscopic inner retinal hyper-reflective phenotypes in retinal and neurologic disease. Invest Ophthalmol Vis Sci. 2014a; 55:4015–29. [PubMed: 24894394]

Scoles D, Sulai YN, Dubra A. In vivo dark-field imaging of the retinal pigment epithelium cell mosaic. Biomedical Optics Express. 2013; 4:1710–23. [PubMed: 24049692]

Scoles D, Sulai YN, Langlo CS, Fishman GA, Curcio CA, et al. In vivo imaging of human cone photoreceptor inner segments. Invest Ophthalmol Vis Sci. 2014b; 55:4244–51. [PubMed: 24906859]

Sharma R, Yin L, Geng Y, Merigan WH, Palczewska G, et al. In vivo two-photon imaging of the mouse retina. Biomed Opt Express. 2013; 4:1285–93. [PubMed: 24009992]

Sredar N, Ivers KM, Queener HM, Zouridakis G, Porter J. 3D modeling to characterize lamina cribrosa surface and pore geometries using in vivo images from normal and glaucomatous eyes. Biomed Opt Express. 2013; 4:1153–65. [PubMed: 23847739]

Stevenson, SB.; Roorda, A. Correcting for miniature eye movements in high resolution scanning laser ophthalmoscopy. In: Manns, F.; Soderberg, P.; Ho, A., editors. Ophthalmic Technologies XI. Bellingham, WA: SPIE; 2005. p. 145-51.

Sulai YN, Dubra A. Non-common path aberration correction in an adaptive optics scanning ophthalmoscope. Biomedical Optics Express. 2014; 5:3059–73. [PubMed: 25401020]

Sulai YN, Scoles D, Harvey Z, Dubra A. Visualization of retinal vascular structure and perfusion with a nonconfocal adaptive optics scanning light ophthalmoscope. J Opt Soc Am A Opt Image Sci Vis. 2014; 31:569–79. [PubMed: 24690655]

Sundaram V, Wilde C, Aboshiha J, Cowing J, Han C, et al. Retinal structure and function in achromatopsia: implications for gene therapy. Ophthalmology. 2014; 121:234–45. [PubMed: 24148654]

Takayama K, Ooto S, Hangai M, Arakawa N, Oshima S, et al. High-resolution imaging of the retinal nerve fiber layer in normal eyes using adaptive optics scanning laser ophthalmoscopy. PLoS One. 2012; 7:e33158. [PubMed: 22427978]

Talcott KE, Ratnam K, Sundquist SM, Lucero AS, Lujan BJ, et al. Longitudinal Study of Cone Photoreceptors during Retinal Degeneration and in Response to Ciliary Neurotrophic Factor Treatment. Invest Ophthalmol Vis Sci. 2011; 52:2219–26. [PubMed: 21087953]

Tam J, Dhamdhere KP, Tiruveedhula P, Manzanera S, Barez S, et al. Disruption of the retinal parafoveal capillary network in type 2 diabetes before the onset of diabetic retinopathy. Invest Ophthalmol Vis Sci. 2011a; 52:9257–66. [PubMed: 22039250]

Tam J, Tiruveedhula P, Roorda A. Characterization of single-file flow through human retinal parafoveal capillaries using an adaptive optics scanning laser ophthalmoscope. Biomed Opt Express. 2011b; 2:781–93. [PubMed: 21483603]

Tuten WS, Tiruveedhula P, Roorda A. Adaptive optics scanning laser ophthalmoscope-based microperimetry. Optometry and Vision Science. 2012; 89:563–74. [PubMed: 22446720]

Vienola KV, Braaf B, Sheehy CK, Yang Q, Tiruveedhula P, et al. Real-time eye motion compensation for OCT imaging with tracking SLO. Biomed Opt Express. 2012; 3:2950–63. [PubMed: 23162731]

Vilupuru AS, Rangaswamy NV, Frishman LJ, Smith EL, III, Harwerth RS, Roorda A. Adaptive optics scanning laser ophthalmoscopy for in vivo imaging of lamina cribrosa. J Opt Soc Am A Opt Image Sci Vis. 2007; 24:1417–25. [PubMed: 17429488]

Wang Q, Tuten WS, Lujan BJ, Holland J, Bernstein PS, et al. Adaptive Optics Microperimetry and OCT Images Show Preserved Function and Recovery of Cone Visibility in Macular Telangiectasia Type 2 Retinal Lesions. Invest Ophthalmol Vis Sci. 2015; 56:778–86. [PubMed: 25587056]

Webb RH, Hughes GW, Pomerantzeff O. Flying spot TV ophthalmoscope. Applied Optics. 1980; 19:2991–97. [PubMed: 20234539]

Weiland JD, Cho AK, Humayun MS. Retinal prostheses: current clinical results and future needs. Ophthalmology. 2011; 118:2227–37. [PubMed: 22047893]

Williams DR. Imaging single cells in the living retina. Vision Research. 2011; 51:1379–96. [PubMed: 21596053]

Xue B, Choi SS, Doble N, Werner JS. Photoreceptor counting and montaging of en-face retinal images from an adaptive optics fundus camera. J Opt Soc Am A Opt Image Sci Vis. 2007; 24:1364–72. [PubMed: 17429482]

Yang Q, Arathorn DW, Tiruveedhula P, Vogel CR, Roorda A. Design of an integrated hardware interface for AOSLO image capture and cone-targeted stimulus delivery. Optics Express. 2010; 18:17841–58. [PubMed: 20721171]

Yannuzzi LA, Bardal AM, Freund KB, Chen KJ, Eandi CM, Blodi B. Idiopathic macular telangiectasia. Archives of Ophthalmology. 2006; 124:450–60. [PubMed: 16606869]

Yin L, Geng Y, Osakada F, Sharma R, Cetin AH, et al. Imaging light responses of retinal ganglion cells in the living mouse eye. J Neurophysiol. 2013; 109:2415–21. [PubMed: 23407356]

Yin L, Masella B, Dalkara D, Zhang J, Flannery JG, et al. Imaging light responses of foveal ganglion cells in the living macaque eye. J Neurosci. 2014; 34:6596–605. [PubMed: 24806684]

Yoon GY, Williams DR. Visual performance after correcting the monochromatic and chromatic aberrations of the eye. Journal of the Optical Society of America A. 2002; 19:266–75.

Zawadzki RJ, Capps AG, Kim DY, Panorgias A, Stevenson SB, et al. Progress on Developing Adaptive Optics-Optical Coherence Tomography for Retinal Imaging: Monitoring and Correction of Eye Motion Artifacts. IEEE journal of selected topics in quantum electronics : a publication of the IEEE Lasers and Electro-optics Society. 2014; 20

Zawadzki RJ, Choi SS, Fuller AR, Evans JW, Hamann B, Werner JS. Cellular resolution volumetric in vivo retinal imaging with adaptive optics-optical coherence tomography. Opt Express. 2009; 17:4084–94. [PubMed: 19259248]

Zayit-Soudry S, Duncan JL, Syed R, Menghini M, Roorda AJ. Cone structure imaged with adaptive optics scanning laser ophthalmoscopy in eyes with nonneovascular age-related macular degeneration. Invest Ophthalmol Vis Sci. 2013; 54:7498–509. [PubMed: 24135755]

Zhang Y, Poonja S, Roorda A. MEMS-based Adaptive Optics Scanning Laser Ophthalmoscope. Optics Letters. 2006; 31:1268–70. [PubMed: 16642081]

Zhang Y, Wang X, Rivero EB, Clark ME, Witherspoon CD, et al. Photoreceptor perturbation around subretinal drusenoid deposits as revealed by adaptive optics scanning laser ophthalmoscopy. American Journal of Ophthalmology. 2014; 158:584–96. [PubMed: 24907433]

Zhong Z, Song H, Chui TY, Petrig BL, Burns SA. Noninvasive measurements and analysis of blood velocity profiles in human retinal vessels. Invest Ophthalmol Vis Sci. 2011; 52:4151–57. [PubMed: 21467177]

Abbreviations

AMD age-related macular degeneration

AOSLO	adaptive optics scanning laser ophthalmoscope
AO	adaptive optics
GC	ganglion cell
NIR	near infra-red
OCT	optical coherence tomography
PSF	point spread function
RP	retinitis pigmentosa
RPE	retinal pigment epithelium
SHWS	Shack-Hartmann wavefront sensor
SNR	signal to noise ratio

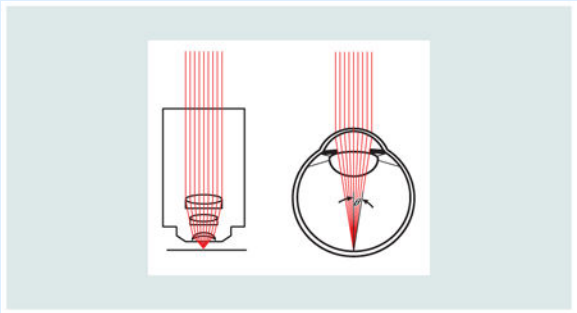

Microscopes and ophthalmoscopes are essentially the same except that in an ophthalmoscope, the eye's optics always serve as the objective lens and the sample is always the retina or other parts of the ocular fundus. The image quality in both are governed by the same rules. Specifically, the numerical aperture, or NA is given by:

$$NA = n \cdot \sin(\theta) = n \cdot sin\left(arctan\left(\frac{D}{2 \cdot f}\right)\right)$$

Where n is the index of refraction of the media in which the light is focused, θ is the half angle of the focused beam at the sample, D is the entrance pupil diameter (beam size) and f is the focal length. Forahuman eye, the NA ranges from 0.03 to 0.2 (1 to 7 mm pupil), whereas microscope optics can be designed with very steep focusing angles, and NAs >1. The resolution (the smallest resolvable distance between two point objects) is related to the NA and often quantified with the equation:

$$R = \lambda / _{2 \cdot NA}$$

An ophthalmoscope can potentially resolve features ∼1.3 microns in size (7 mm beam, 550 nm light), whereas a microscope with a **NA** of 1 can resolve 0.275 microns. However, this equation applies to diffraction-limited systems only (a system where the only limit to resolution is the diffraction of light). Aberrations in the eye make an opthalmoscope's resolving power much worse, which is why adaptive optics are needed.

There are three metrics that can be used to define the quality of an image; resolution, contrast, and signal to noise ratio (SNR).

Resolution is the ability of an imaging system to allow two adjacent structures to be visualized as being separate, or the distinctness of an edge in the image (ie, sharpness).

Contrast is the difference in luminance and/or color that makes an object (or its representation in an image or display) distinguishable.

SNR is the ratio of the power between the signal strength and the background noise.

The following three figures of a letter E against a background illustrate the differences.

Although they can be considered independently, they are related. For example, improved resolution (offered by AO) will improve the contrast of higher frequencies, thereby increasing overall contrast and signal to noise. But an image of an object with low contrast and/or low SNR may never be visualized, no matter how high the resolution.

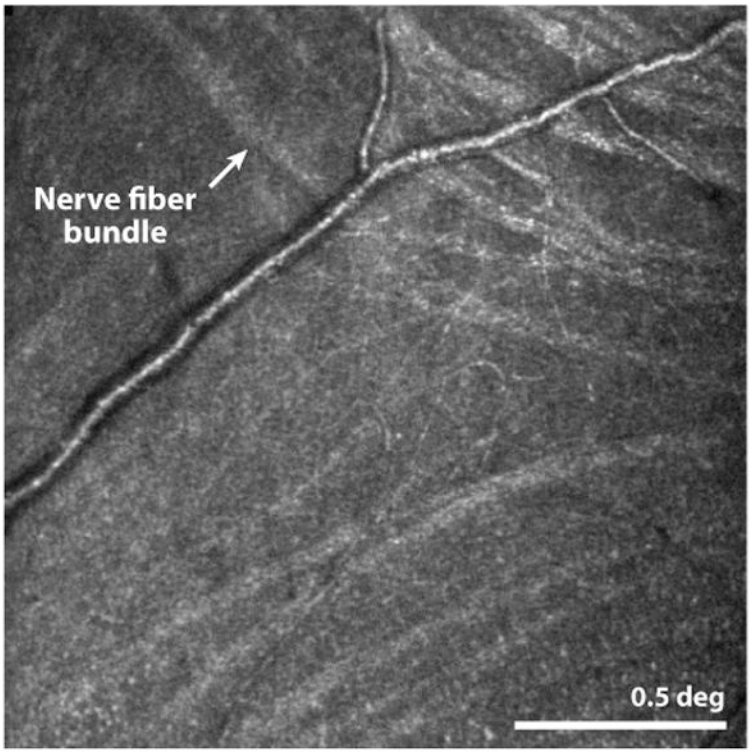

Figure 1.

(Huang et al 2014) This confocal AOSLO image shows the location where nerve fiber bundles originate temporal to the fovea. The line separating bundles that traverse above and below the fovea is the called the temporal raphe. In the original paper, the authors carefully map its location relative to the fovea and optic disk and show individual variability and changes with age. Scale bar is 0.5 deg.

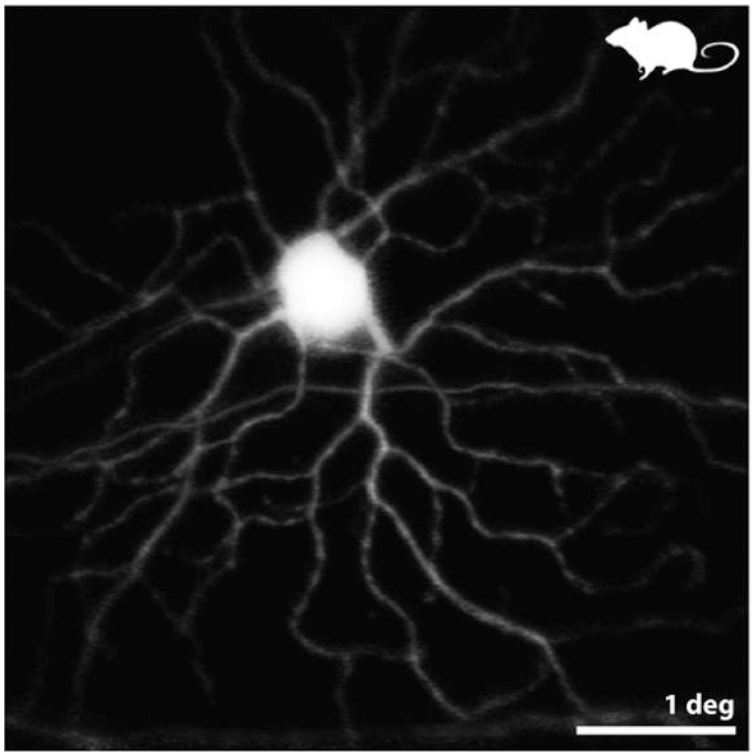

Figure 2.

from (Geng et al 2012) Fluorescence AOSLO images of the retina of a living mouse expressing YFP in a fraction of its GCs. This pair of images shows a monostratified ON GC. ON or OFF types were identified by resolving – through confocal optical sectioning – the sublamina of the dendrites within the inner plexiform layer. Scale bar is 1 deg (∼ 30 microns).

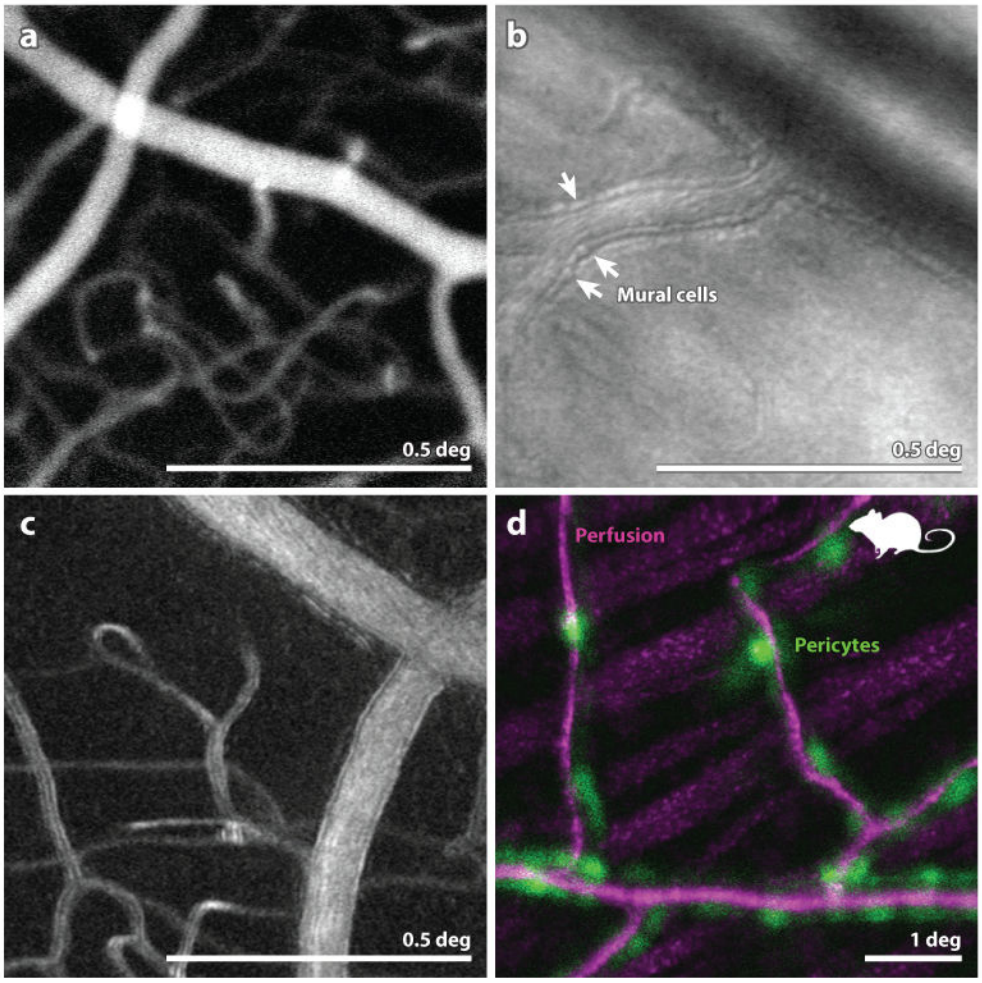

Figure 3.

(A) (from (Pinhas et al 2013)) Fluorescein angiography with AOSLO. This particular implementation employed oral fluorescein, offering a longer time course for imaging and avoiding risks associated with injection. The use of AOSLO offers higher contrast and higher resolution over conventional FA. (B) from (Chui et al 2013) Image of the microvascular structure using offset-pinhole AOSLO. Arrowheads point to purported individual mural cells comprising the arteriole walls. (C) from (Sulai et al 2014) Motion contrast image from split-detector AOSLO recordings of a vessel and capillary network in a normal eye. The scale bar is 0.5 deg and applies to panels (A) (B) and (C). (D): from (Schallek et al 2013) A combination of confocal AOSLO motion contrast of perfusion (magenta) and fluorescent AOSLO images of tagged pericytes (green) in a mouse retina reveals the colocation of these structures. Scale bar is 1 deg.

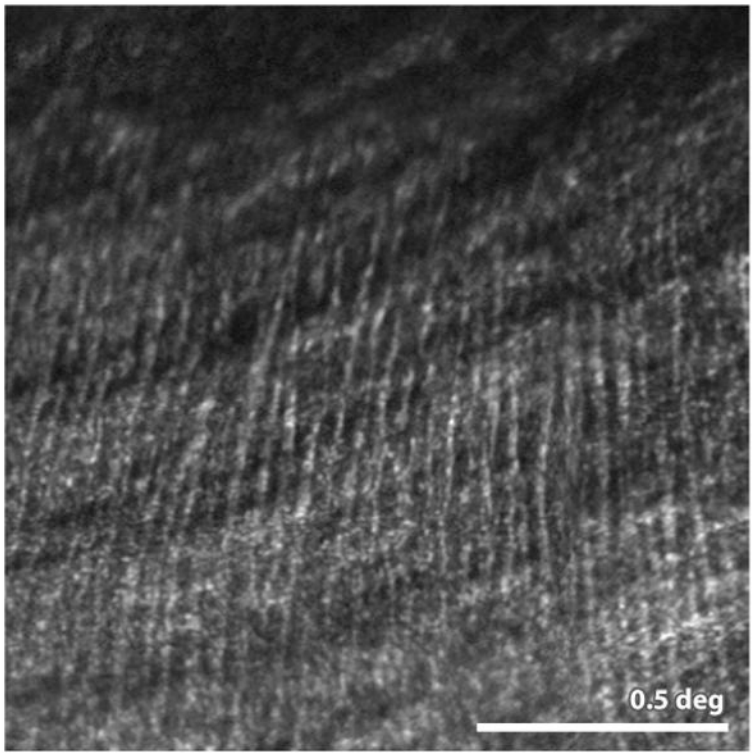

Figure 4.
(Scoles et al 2014a) Confocal AOSLO image of a patients with Best's disease. Purported Henle fibers are running vertically across most of the image. Larger more horizontally-oriented structures are from the NFL. Scale bar is 0.5 deg.

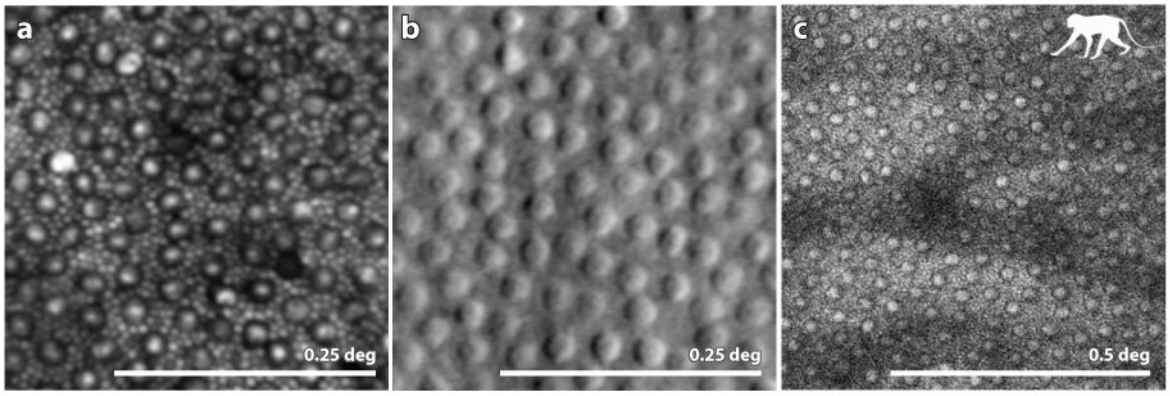

Figure 5.

(A) from (Cooper et al 2011): confocal AOSLO image of a healthy human retina showing a complete mosaic of cones (large cells) and rods (intervening smaller cells) at a location 10 deg temporal to the fovea. **(B)** from (Scoles et al 2014b) Split detector AOSLO image of a healthy human retina showing an array of cone inner segments at a location 10 deg from the fovea. Owing to their small size the rods, which fill the intervening space between the cones at this location, are too small to be resolved. **(C)** (courtesy of Jennifer Hunter, Robin Sharma and David Williams) 2-photon fluorescence AOSLO image of the retina of a macaque monkey showing the array of inner segments (confirmed by taking a confocal AOSLO image at the same location). The mosaic in the 2-photon image indicates that the fluorophores are contained within each inner segment. Scale bar is 0.25 deg for panels A and B and 0.5 deg for panel C.

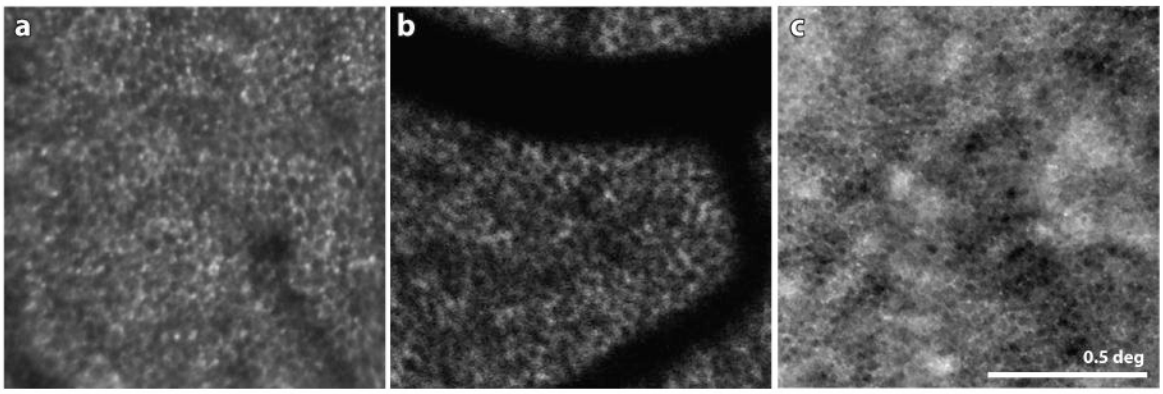

Figure 6.

(A) Confocal AOSLO image of the RPE mosaic at a location 3 deg inferior to the fovea in a patient with autosomal dominant RP. The lack of overlying visible or functional photoreceptors in this region allowed the RPE cells to be seen. **(B)** from (Morgan et al 2009) AOSLO fundus autofluorescence image of a healthy human retina. By resolving the FAF signal, the mosaic of RPE cells is readily visible. The dark shadows in this panel are shadows cast by the overlying blood vessels. The FAF uses short wavelength light in both directions, which is especially susceptible to absorption by the overlying blood vessels (see Sec 5.1 for more discussion). **(C)** from (Scoles et al 2013) Dark field AOSLO image of a foveal RPE mosaic in a healthy human retina. The same location imaged in confocal AOSLO mode shows a complete mosaic of photoreceptors. Scale bar is 0.5 deg.

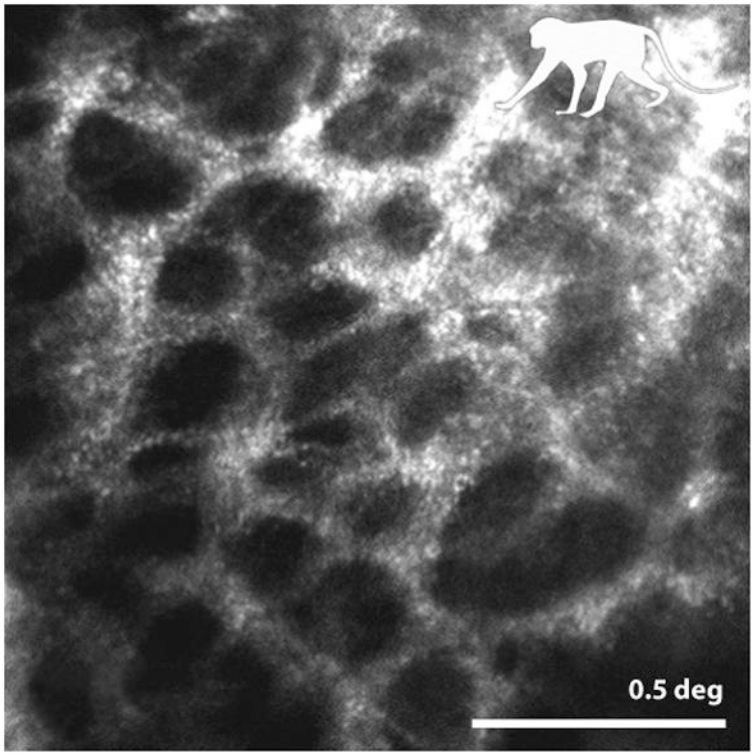

Figure 7.

from (Ivers et al 2011) Detailed image of the collagen beams comprising the inner surface of the lamina cribrosa in a non-human primate. Morphometric analysis of LC pore size and pore elongation have been found to be sensitive to change in ocular pressure in animal models. Scale bar is 0.5 deg.

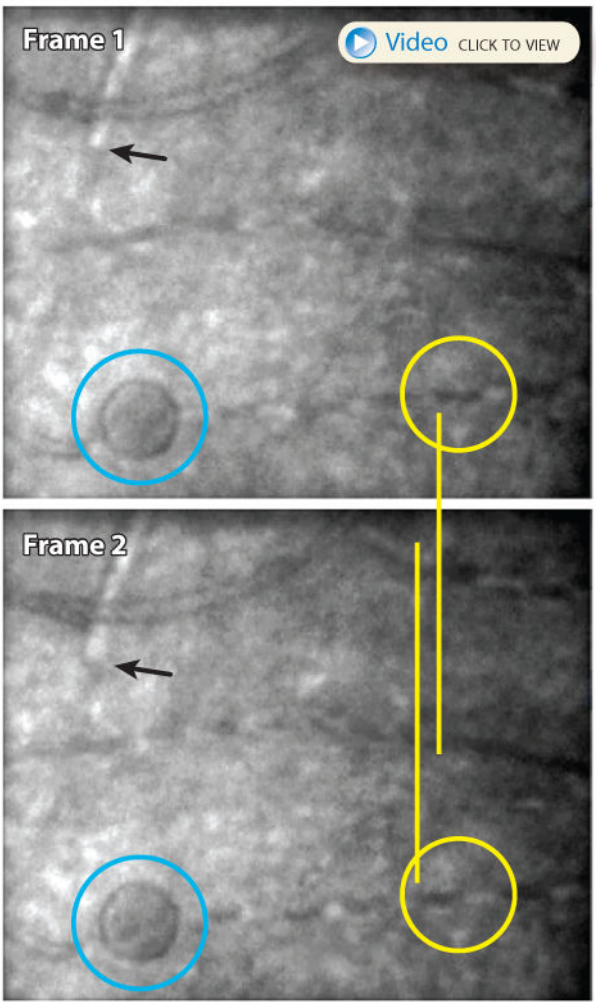

Figure 8.

(courtesy of Phil Bedggood and Andrew Metha, University of Melbourne) The upper two panels show two subsequent frames from a 400 fps AO fundus camera video of a patient with type 1 diabetes. One of the hyporeflective red blood cells in frame 1 is circled in yellow. The same cell appears in the next frame displaced to the left. A white blood cell in the upper left of each frame (black pointer) shows similar movement. The blue circle indicates a microcyst which resides in the same plane as the vasculature. The slow-moving blood cells are much better appreciated in the video.

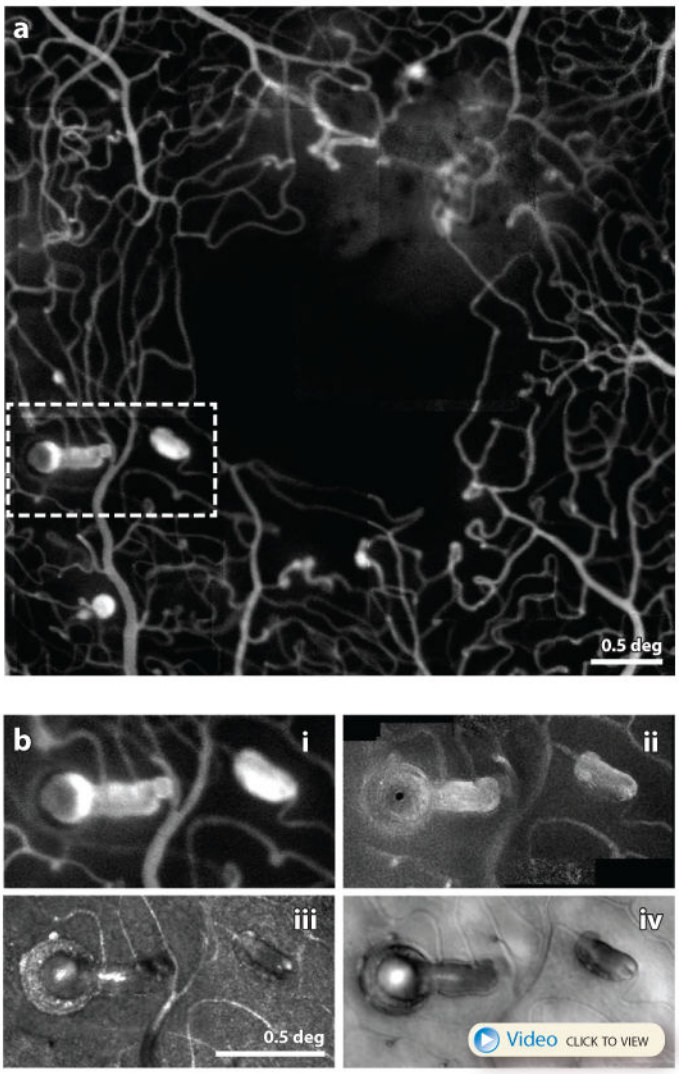

Figure 9.

(A) adapted from (Dubow et al 2014) AOSLO fluorescein angiography image of a patient with hypertension. A myriad of microaneurysm types are seen here along with the fine details of the associated microcapillary network. Scale bar is 0.5 deg. **(B)** from (Chui et al 2014) This figure shows a close up of one location indicated by the dashed white box in (A) imaged using in 4 different modes in the same AOSLO system **(B.i)** fluorescein angiography **(B.ii)** confocal **(B.iii)** motion contrast **(B.iv)** offset pinhole. A video recorded with offset pinhole AOSLO can be seen here. Collectively they represent the most detailed characterization of single microaneurysm from a human eye in history. Scale bar is 0.5 deg.

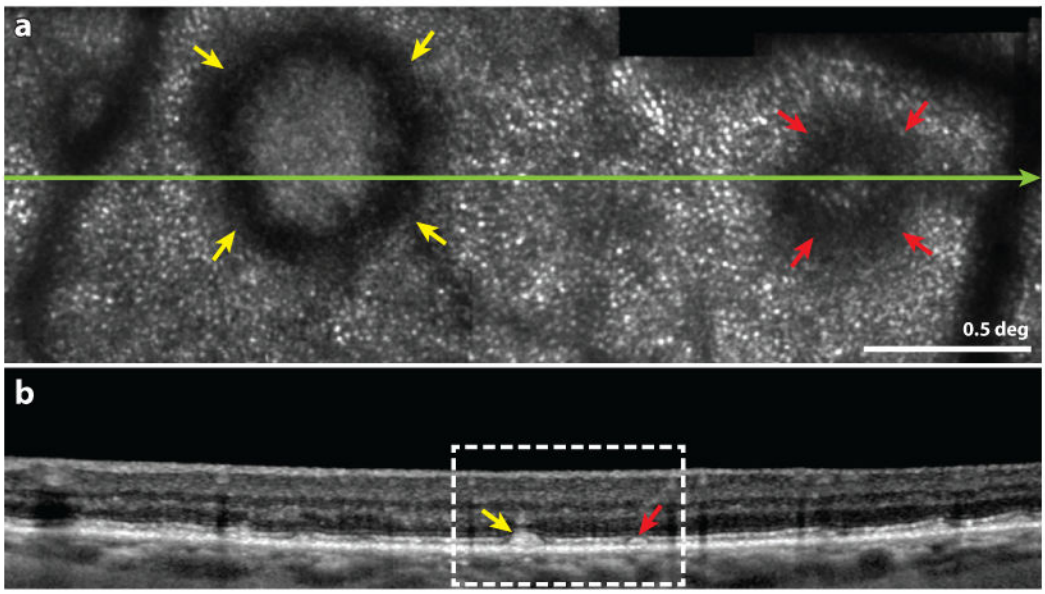

Figure 10.

from (Zhang et al 2014) Multimodal imaging of subretinal drusenoid deposits (SDD, or pseudodrusen) in a patient with AMD. **Upper frame**: Confocal AOSLO image. The yellow and red arrowheads indicate prominent stage 3 and stage 2 SDDs, characterized by a hyporeflective ring and no discernible cones over the SDD. Normal appearing cones are resolved outside of the SDD. The green line indicates the location of the OCT b-scan shown in the lower frame. Scale bar is 0.5 deg. **Lower frame**: SD-OCT b-scan showing a wider field image of the same structure. The white box indicates the region in the AOSLO image in the upper frame.

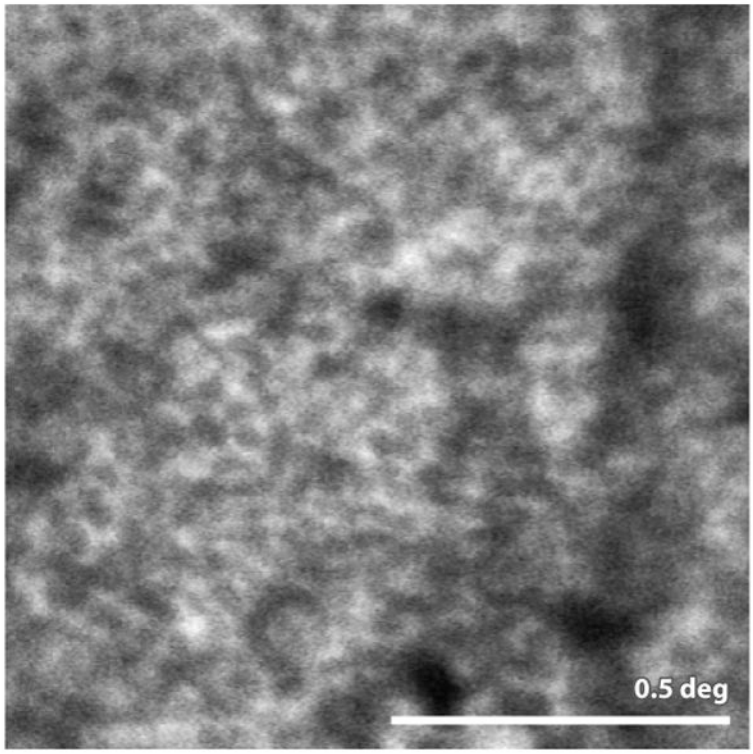

Figure 11.
from (Rossi et al 2013) AOSLO autofluorescence image of the RPE mosaic in a patient with AMD. Analysis of this mosaic and other mosaic from AMD patients showed that the RPE regularity is disrupted in this disease. Scale bar is 0.5 deg.

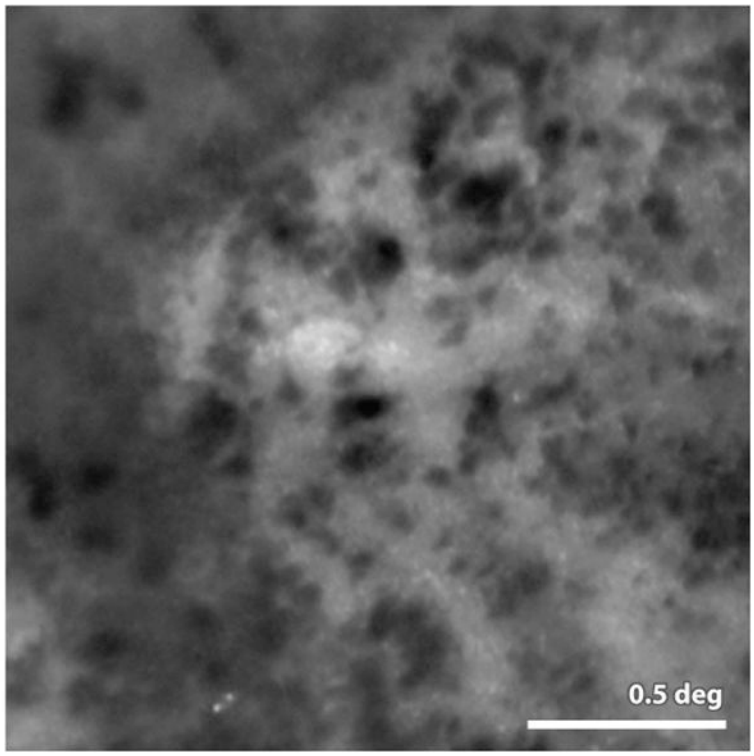

Figure 12.

from (Gocho et al 2013) Image of melanin granules taken with an AO fundus camera (rtx1, Imagine Eyes Inc. Orsay France). The granules are readily visible in AMD patients in the vicinity of geographic atrophy (lighter background regions in the image) the authors report that these granules are highly active, appearing and disappearing and moving many microns over the course of weeks. Scale bar 0.5 deg

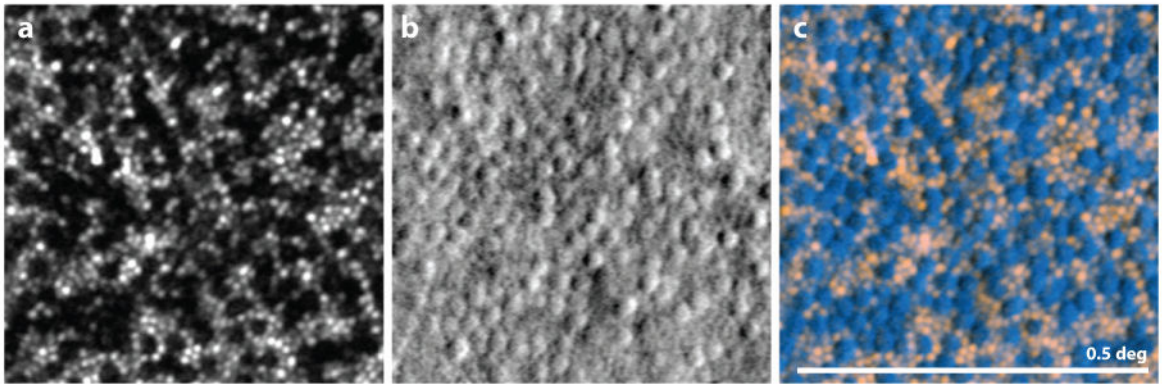

Figure 13.

from (Scoles et al 2014b) Image showing the value of split detector imaging for prescreening patients. All images are from the same location of a single patient with achromatopsia. (A) Confocal AOSLO image. Holes are present where the cones might normally reside. The visible spots are from intact, functional rods. (B) Split-detector AOSLO, where a mosaic of structures is present, presumably the inner segments of the cones. (C) Overlay of the confocal image (pink) with the split detector image (blue) revealing that the mosaic of cells corresponds directly with the gaps in the mosaic from the left image. In this case, it appears that although the cones are dysfunctional in this patient, there is a mosaic of inner segments present. It is suggested that patients with this phenotype are most likely to benefit from gene therapy. Scale bar is 0.5 deg.

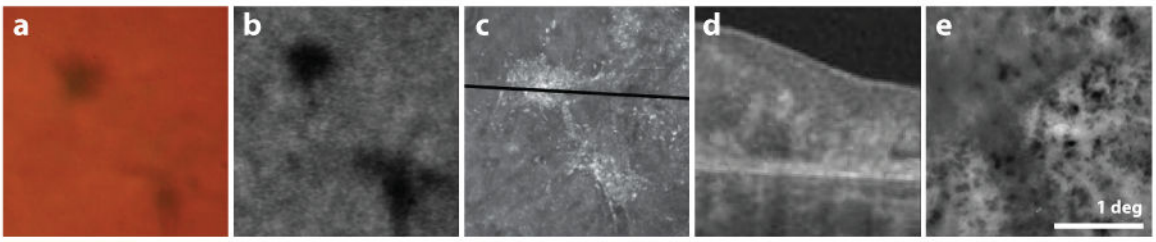

Figure 14.

Images of melanin pigment taken using five different imaging modalities. The first four panels show registered images from a single patient with idiopathic macular telangiectasia type 2, the last frame is cropped from Fig. 12. Color fundus photo: pigment appears dark and brownish in color; FAA from Heidelberg Spectralis: pigment appears dark; AOSLO: pigment is hyperreflective in NIR (840 nm); OCT b-scan (scan location indicated in previous panel) pigment is hyper-reflective in NIR (∼840 nm); AO fundus: pigment is hyporeflective. Scale bar is 1 deg.